HEALTH AND MEDICINE

Engineered immunomodulatory accessory cells improve experimental allogeneic islet transplantation without immunosuppression

Xi Wang[1], Kai Wang[2,3], Ming Yu[4], Diana Velluto[5], Xuechong Hong[2,3], Bo Wang[1], Alan Chiu[1], Juan M. Melero-Martin[2,3,6], Alice A. Tomei[5,7,8], Minglin Ma[1]*

Islet transplantation has been established as a viable treatment modality for type 1 diabetes. However, the side effects of the systemic immunosuppression required for patients often outweigh its benefits. Here, we engineer programmed death ligand-1 and cytotoxic T lymphocyte antigen 4 immunoglobulin fusion protein–modified mesenchymal stromal cells (MSCs) as accessory cells for islet cotransplantation. The engineered MSCs (eMSCs) improved the outcome of both syngeneic and allogeneic islet transplantation in diabetic mice and resulted in allograft survival for up to 100 days without any systemic immunosuppression. Immunophenotyping revealed reduced infiltration of $CD4^+$ or $CD8^+$ T effector cells and increased infiltration of T regulatory cells within the allografts cotransplanted with eMSCs compared to controls. The results suggest that the eMSCs can induce local immunomodulation and may be applicable in clinical islet transplantation to reduce or minimize the need of systemic immunosuppression and ameliorate its negative impact.

INTRODUCTION

Type 1 diabetes (T1D) is an autoimmune disease in which immune cells (mainly $CD8^+$ T cells) mistakenly attack β cells, causing deficiency of insulin and elevation of blood glucose. Replacement of β cells by allogeneic islet transplantation via portal vein has been established in clinics all over the world and shown to improve glycemic control among patients (*1*, *2*). However, systemic immunosuppression, required to prevent allograft rejection, may be toxic to islets and, more importantly, has deleterious side effects to patients (*3*, *4*). Of note, for most T1D patients, the systemic immunosuppression is riskier than long-term standard management with exogenous insulin supplementation, which makes eliminating systemic immunosuppression critical to β cell replacement therapies. Novel strategies to circumvent the challenges associated with systemic immunosuppression have been extensively pursued for islet transplantation recently including immunoprotection using cell encapsulation devices (*5*–*8*) and induction of local immunotolerance toward allogeneic islets (*9*). Compared to cell encapsulation, the local immunomodulation approach is considered as "open," involving no physical barrier between the graft and the body and therefore can potentially allow better and direct host integration.

In general, T cells play a critical role in allograft rejection (*10*, *11*). Upon recognition of alloantigens, a costimulatory signal, commonly provided by B7-1 (CD80) or B7-2 (CD86) ligands on antigen-presenting cells (APCs) that interact with CD28 on T cells, is necessary for T cell activation (*9*). Thus, modulation of T cell costimulatory pathways, including blocking T cell costimulation and/or providing negative modulatory signals, has been investigated and used to improve graft survival and functionality. Specifically, the programmed death-1 (PD-1)/programmed death ligand-1 (PD-L1) interaction is a well-studied negative costimulatory pathway, which is critical in maintaining peripheral tolerance and immunological homeostasis (*12*). Targeting the PD-1/PD-L1 pathway was shown to regulate and delay immune destruction of allograft in cardiac (*13*, *14*), islet (*15*), and corneal (*16*) transplantation. Similarly, the cytotoxic T lymphocyte antigen 4 immunoglobulin (CTLA4-Ig) fusion protein, which competitively blocks the CD28-B7 pathways, was shown to inhibit T cell activation (*17*) and prevent allograft rejection in skin (*18*), cardiac (*19*, *20*), liver (*21*), and islet (*22*, *23*) transplantation. In addition, PD-L1 and CTLA4-Ig have been demonstrated to inhibit T cell activity in a nonredundant way (*24*, *25*). Despite these promising developments, the PD-L1 or CTLA4-Ig was often administered systemically and cause nonspecific immune responses and immune-related toxicity (*26*). Thus, there is great interest in targeted delivery of immunomodulatory molecules and localized regulation of immune responses within the graft microenvironment.

Multiple studies have reported strategies of using the PD-L1 or CTLA4 immune checkpoint pathways to improve islet transplantation in a localized manner. For example, researchers engineered functional biomaterial platforms [poly(ethylene glycol) (PEG) microgels] to display PD-L1, which have been shown to achieve long-term allogeneic islet graft function in diabetic mouse models with a short-term (15 days) administration of rapamycin (*27*). A major advantage of the biomaterial approach is that the biomaterial can be prefabricated, and there is a minimal need, if any, to manipulate or modify the islets. However, biomaterials can cause foreign body responses and induce antibodies (e.g., anti-PEG antibodies) and may be challenging to be applied in current clinical islet transplantation through the portal vein. In addition, the immunomodulatory ligands delivered or presented via biomaterials may degrade or be depleted over time. Alternatively, mouse islets were modified with PD-L1/CTLA4-Ig (*28*) or PD-L1 (*29*, *30*), which resulted in protection of islets from acute rejection. Although modifying islets is a straightforward

[1]Department of Biological and Environmental Engineering, Cornell University, Ithaca, NY 14853, USA. [2]Department of Cardiac Surgery, Boston Children's Hospital, Boston, MA 02115, USA. [3]Department of Surgery, Harvard Medical School, Boston, MA 02115, USA. [4]Department of Surgery, Hospital of the University of Pennsylvania, Philadelphia, PA 19104, USA. [5]Diabetes Research Institute, University of Miami Miller School of Medicine, Miami, FL 33136, USA. [6]Harvard Stem Cell Institute, Cambridge, MA 02138, USA. [7]Department of Biomedical Engineering, University of Miami, Miami, FL 33146, USA. [8]Department of Surgery, University of Miami Miller School of Medicine, Miami, FL 33136, USA.
*Corresponding author. Email: mm826@cornell.edu

approach, the modification takes time and may be challenging to be applied in clinical settings, especially given that human islets are not easy to maintain in vitro for a long time.

Overcoming these challenges and developing an approach that protects the graft locally require no modification of islets and may be compatible with current clinical islet transplantation; thus, we engineered mesenchymal stromal cells (eMSCs) with overexpression of both PD-L1 and CTLA4-Ig as accessory cells for islet cotransplantation (Fig. 1A). The eMSCs suppressed activation and proliferation of allogeneic and diabetogenic $CD4^+$ and $CD8^+$ T cells in vitro after 3 days of coculture. The immunomodulatory function of the PD-L1 and CTLA4-Ig expression was further confirmed by delayed rejection of similarly engineered allogeneic 4T1 cells in immunocompetent mice. The therapeutic potential of the eMSCs was demonstrated in two scenarios of islet transplantation (Fig. 1B). In an allogeneic mouse transplantation model, islets transplanted with the eMSCs in kidney capsules functioned and corrected diabetes for up to 100 days without any systemic immunosuppression, while islets transplanted with unmodified MSCs or alone were rejected by days 20 and 14, respectively. Even in a syngeneic model, the eMSCs prolonged and enhanced the islet function, likely due to their anti-inflammatory and paracrine effects. Immunological profiling of explanted allografts with or without eMSCs showed that the eMSCs reduced the infiltration of $CD4^+$ or $CD8^+$ T effector (T_{eff}) cells and promoted graft infiltration of regulatory T (T_{reg}) cells within the graft microenvironment. We also confirmed that the immunomodulatory effect was local as allogeneic islets transplanted in the other kidney capsule of the same mouse were still rapidly rejected. Our results in mice suggest that PD-L1/CTLA4-Ig–expressing eMSCs can immunologically protect cotransplanted islets and may be applicable as accessory cells in clinical islet transplantation to improve graft function, minimize systemic immunosuppression, and ameliorate its negative impact.

RESULTS

Engineering and characterizations of MSCs expressing PD-L1 and CTLA4-Ig

MSCs derived from bone marrow of C57BL/6 mice were chosen as starting cells because MSCs exist abundantly in multiple tissues and have been shown to be promising in multiple therapeutic applications (*31*). Before modification, the MSCs were positive for mesenchymal stromal cell markers such as CD29 (99%), SCA-1 (94.4%), and CD44 (99.7%) and negative with CD31 (0.033%), CD45 (0.0065%), and CD117 (0.086%) (fig. S1). The eMSCs expressing PD-L1 and CTLA4-Ig were generated by transfection using lentivirus carrying targeted genes (mouse PD-L1 and CTLA4-Ig) and selection through antibiotic blasticidin (Bsd) (Fig. 2A). Gene expression of *PD-L1* and *CTLA4-Ig* demonstrated that both genes were incorporated into the genome and highly expressed in the eMSCs, with a 500-fold and 800-fold change compared to MSCs, respectively (Fig. 2B). In the meantime, cell modification did not alter the gene expression of other selected molecules examined such as transforming growth factor β1, arginase 1, inducible nitric oxide synthase, and tumor necrosis factor–α (fig. S2) in eMSCs compared to MSCs ($P > 0.05$). Western blot analysis with specific anti–PD-L1 and anti–CTLA4 antibodies verified PD-L1 (55 kDa) and CTLA4 (62 kDa) expressions in the eMSCs (Fig. 2C). Using enzyme-linked immunosorbent assay (ELISA), CTLA4-Ig was detected in the culture medium of eMSCs after in vitro culture for 6 hours, while no CTLA4-Ig was detected in that of MSCs, confirming the secretion of CTLA4-Ig as a soluble factor by the eMSCs (Fig. 2D). Flow cytometry showed that 97.1% eMSCs expressed both CD29 and PD-L1 markers, while almost no expression of PD-L1 was detected on MSCs (Fig. 2E). Immunofluorescent staining images further confirmed the expression of PD-L1 on eMSCs but not MSCs (Fig. 2F).

After verification of PD-L1 and CTLA4-Ig expression by eMSCs, we investigated their ability to suppress T cell function via an in vitro T cell proliferation and activation assay. We cocultured allogeneic and diabetogenic splenocytes isolated from either transgenic BDC2.5 nonobese diabetic (NOD) mice [CD4 T cells with transgenic T cell receptor (TCR) specific for the BDC2.5 mimotope presented on MHCII] or from transgenic NY8.3 NOD mice [CD8 T cells with transgenic TCR specific for the islet-specific glucose-6-phosphatase catalytic subunit-related protein (IGRP) peptide presented on MHCI], labeled with a cell proliferation dye (CellTrace) and pulsed with either the BDC2.5 mimotope or the IGRP peptide, with MSCs or eMSCs at a ratio of 5:1 (splenocytes:MSCs), followed by flow cytometry analysis of T cell proliferation and activation, respectively. The data indicated that more than 80% of CD4 T cells and CD8 T cells proliferated when splenocytes were stimulated by the BDC2.5 mimotope and the IGRP peptide, respectively (Fig. 2, G to J). While MSCs did not have an effect on either CD4 or CD8 T cell proliferation, eMSCs suppressed the proliferation of both $CD4^+$ and $CD8^+$ allogeneic and diabetogenic T cells compared to MSCs (Fig. 2, G to J). Quantitative

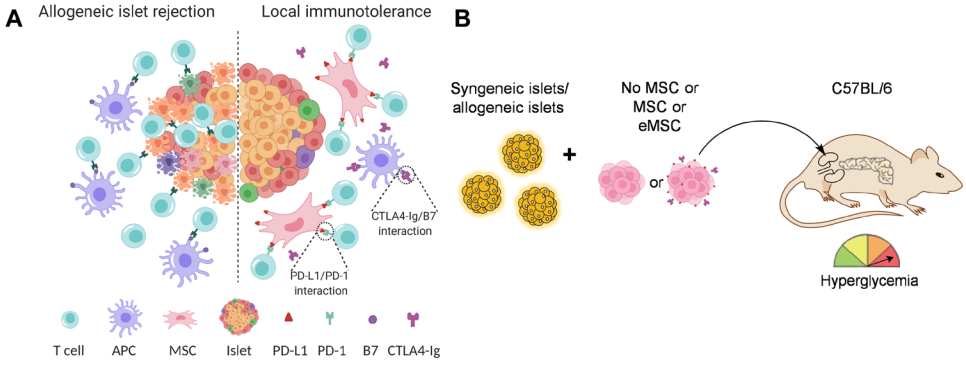

Fig. 1. Schematics of local immunotolerance induction by eMSCs. (**A**) Local immunomodulation with eMSCs expressing PD-L1 and CTLA4-Ig protects allogeneic islets from being rejected. (**B**) Experimental design of animal studies showing the syngeneic or allogeneic islets without MSCs, with MSC spheroids, or with eMSC spheroids that were transplanted into diabetic C57BL/6 mice in the kidney capsule.

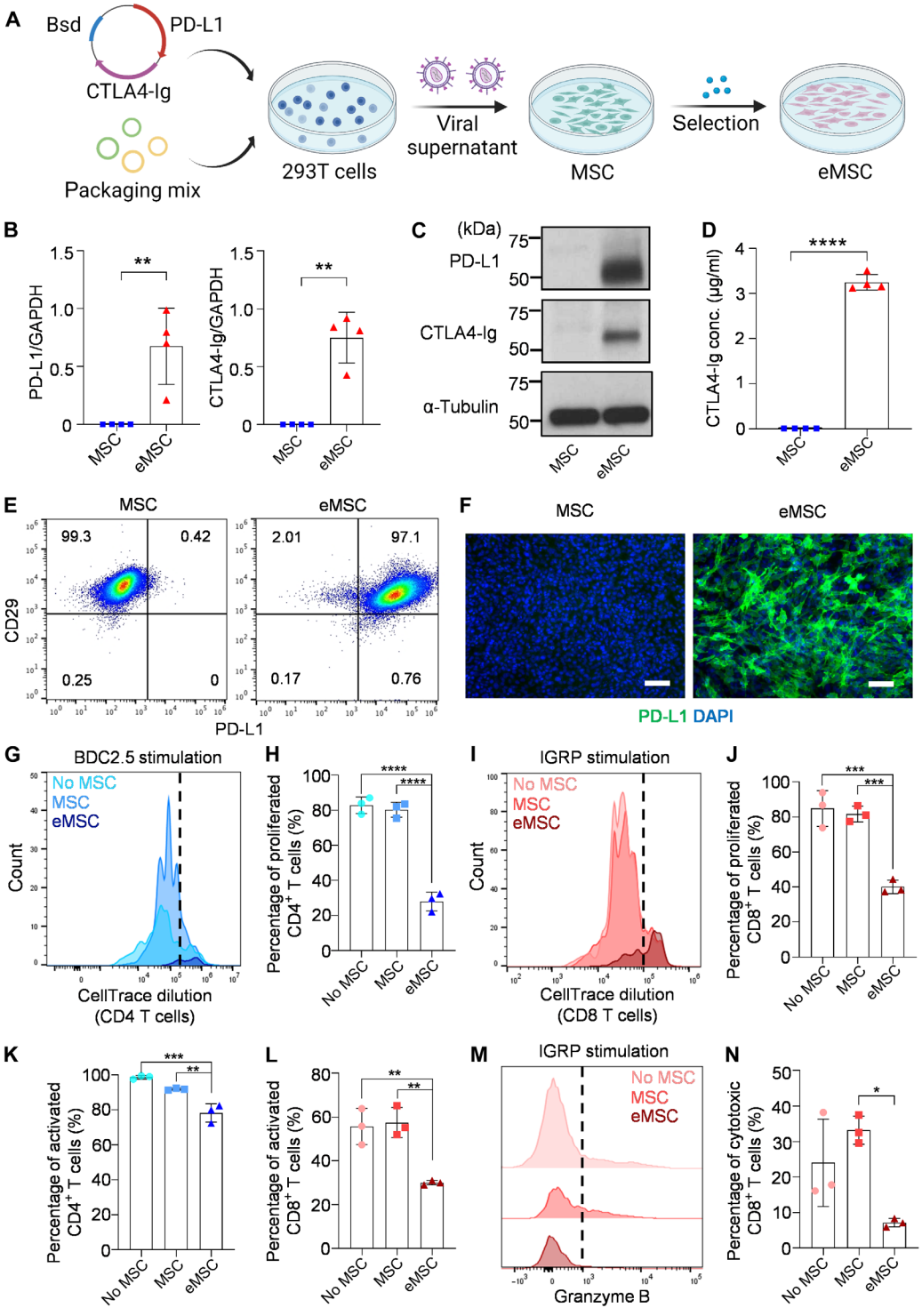

Fig. 2. In vitro characterization of eMSCs expressing PD-L1 and CTLA4-Ig. (**A**) Experimental outline for generating eMSCs. (**B**) mRNA expression of PD-L1 and CTLA4-Ig in MSCs and eMSCs (normalized to GAPDH expression) ($n = 4$). (**C**) Western blot analysis of PD-L1 and CTLA4-Ig in MSCs and eMSCs. (**D**) The concentration of CTLA4-Ig in the culture medium of MSCs and eMSCs ($n = 4$). (**E**) Flow cytometric plots of MSCs and eMSCs stained for CD29 and PD-L1. (**F**) Immunofluorescent staining of MSCs and eMSCs with antibodies (green, PD-L1; blue, DAPI). (**G**) In vitro $CD4^+$ T cell proliferation as measured by CellTrace dilution. (**H**) Quantitative analysis of proliferated $CD4^+$ T cell percentage shown in (G) ($n = 3$). (**I**) In vitro $CD8^+$ T cell proliferation as measured by CellTrace dilution. (**J**) Quantitative analysis of proliferated $CD8^+$ T cell percentage shown in (I) ($n = 3$). (**K**) Quantitative analysis of activated $CD4^+$ T cell percentage ($n = 3$). (**L**) Quantitative analysis of activated $CD8^+$ T cell percentage ($n = 3$). (**M**) Flow cytometry plots of T cells stained with CD8 and granzyme B. (**N**) Quantitative analysis of cytotoxic $CD8^+$ T cell percentage shown in (M). The two-tailed Student's *t* test was performed when the data consisted of only two groups. One-way ANOVA followed by Tukey's test was performed for comparing the multigroup data. The level of significance was labeled by *, **, ***, and ****, denoting *P* values of <0.05, <0.01, <0.001, and <0.0001, respectively. Scale bars, 100 μm (F).

analysis confirmed the proliferation inhibition of both allogeneic and diabetogenic $CD4^+$ and $CD8^+$ T cells when cocultured with eMSCs (Fig. 2, H and J). Similarly, stimulated by the BDC2.5 mimotope or the IGRP peptide, more than 95% CD4 T cells and around 55% CD8 T cells were highly activated as upregulation of CD25 and CD44 (Fig. 2, K and L, and fig. S3). While MSCs did not have an influence on either CD4 or CD8 T cell activation, eMSCs significantly reduced the percentage of activated CD4 T cells ($CD4^+CD25^+CD44^+$) and activated CD8 T cells ($CD8^+CD25^+CD44^+$) compared to the no-MSC and MSC groups ($P < 0.01$) (Fig. 2, K and L, and fig. S3). Furthermore, cytotoxic $CD8^+$ T cells were identified by their expression of granzyme B. The data showed that around 24 and 33.2% of CD8 T cells were granzyme B^+ after IGRP stimulation in the no-MSC and MSC groups, respectively (Fig. 2, M and N, and fig. S3). In contrast, around 7.1% CD8 T cells showed a cytotoxic phenotype as granzyme B expression in the eMSC group. Thus, eMSCs significantly inhibited cytotoxic CD8 T cell generation ($CD8^+$ granzyme B^+) compared to MSCs ($P < 0.05$) (Fig. 2, M and N, and fig. S3).

PD-L1 and CTLA4-Ig expression delays allogeneic cell rejection

To evaluate whether the PD-L1 and CTLA4-Ig expression itself can protect allogeneic cells from immune rejection, we transfected 4T1 cells from BALB/c mice, a common and robust cell line, with two lentivirus vectors carrying green fluorescent protein (GFP)/luciferase and PD-L1/CTLA4-Ig, respectively. The GFP/luciferase 4T1 cells were first generated (fig. S4A) and then modified with PD-L1/CTLA4-Ig. Flow cytometry revealed that around 91% of modified cells overexpressed PD-L1, while only 3% of native 4T1 cells had PD-L1 expression (Fig. 3A). The GFP/luciferase-expressing 4T1 cells, with or without PD-L1/CTLA4-Ig expression, were transplanted in the right hindlimbs of healthy allogeneic C57BL/6 mice, and their survival was compared through bioluminescent imaging. The results showed that 4T1 cells without PD-L1/CTLA4-Ig expression were rejected within 14 days after transplantation in all C57BL/6 recipients (five of five), while PD-L1/CTLA4-Ig–expressing 4T1 cells survived in four of five animals at 14 days after transplantation, with one that survived for as long as 60 days (Fig. 3, B and C). The survival curve indicated that expression of PD-L1 and CTLA4-Ig significantly delayed allorejection (Fig. 3D), with a median survival time of 21 days ($P < 0.05$).

A 4T1 tumor was formed in the hindlimb of allogeneic mouse 60 days after the injection of modified 4T1 cells (Fig. 3E). As control, GFP/luciferase-expressing native 4T1 cells were injected into the hindlimb of syngeneic BALB/c mice (fig. S4, B and C), which

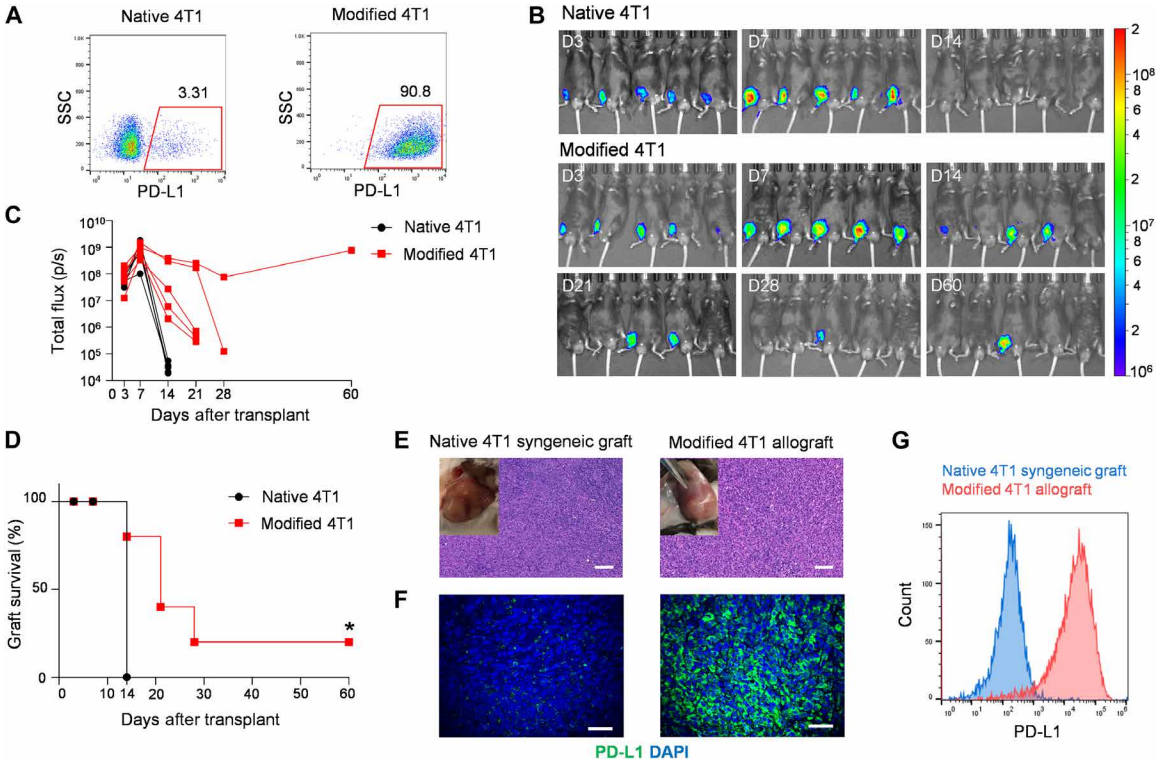

Fig. 3. Expression of PD-L1 and CTLA4-Ig in 4T1 breast cancer cells delays allorejection. (**A**) Flow cytometric dot plots of native 4T1 and modified 4T1 stained for PD-L1. (**B**) Bioluminescent images of healthy C57BL/6 mice transplanted with native 4T1 cells and modified 4T1 cells (derived from fully MHC-mismatched BALB/c) in right hindlimb ($n = 5$). (**C**) Quantitative analysis of the bioluminescent intensity of the engrafted cells shown in (B). Each line represents one mouse ($n = 5$). (**D**) Graft survival curve of healthy C57BL/6 mice receiving native 4T1 and modified 4T1 cells. (**E**) Representative H&E staining images of native 4T1 cells engrafted in syngeneic BALB/c mice (left) and modified 4T1 cells engrafted in allogeneic C57BL/6 mice (right). Representative digital images of 4T1 tumor grown in syngeneic and allogeneic mice in the right hindlimb are shown in the inset. (**F**) Representative immunofluorescent images of native 4T1 cells engrafted in syngeneic BALB/c mice (left) and modified 4T1 cells engrafted in allogeneic C57BL/6 mice (right) stained with antibodies (green, PD-L1; blue, DAPI). (**G**) Flow cytometry analysis of native 4T1 cells isolated from the tumor grown in syngeneic mice and modified 4T1 cells isolated from long-term grafts in allogeneic mice after 60 days with PD-L1 marker. Survival curve was analyzed using a Mantel-Cox test. The level of significance was labeled by *, denoting a P value of <0.05. Scale bars, 50 μm (F) and 100 μm (E).

also formed a tumor (Fig. 3E). The morphology of the 4T1 tumor engrafted in the allogeneic C57BL/6 mouse was similar to that of the tumor formed by native 4T1 cells in the syngeneic BALB/c mouse at 60 days (Fig. 3E). Immunofluorescent staining showed that most of the cells within the modified 4T1 allograft were stained with PD-L1, while very few cells within the native 4T1 syngeneic graft expressed PD-L1 (Fig. 3F). Both the allograft and syngeneic graft cells were isolated from the tumor and further analyzed by flow cytometry. Not unexpectedly, 90.3% of engrafted cells expressed PD-L1, while only 0.8% of native 4T1 cells were positive with PD-L1 expression (Fig. 3G). Together, these data demonstrated that the expression of PD-L1 and CTLA4-Ig itself delayed allorejection.

PD-L1/CTLA4-Ig–overexpressing MSCs improve syngeneic islet transplantation

After confirming the immunomodulatory effects of PD-L1/CTLA4-Ig expression in allogeneic cells, we started to explore the therapeutic potential of the eMSCs as protective accessory cells in islet transplantation. First, we examined the in vitro biocompatibility of the eMSCs with islets by coculturing mouse islets with MSCs or eMSCs for 24 hours (fig. S5A), using islets cultured alone as control. The live and dead imaging and quantitative analysis of fluorescence intensity demonstrated that there was no difference in terms of the viability of the islets among the three groups (Fig. 4, A and B). Furthermore, to test the function of islets after coculture, the glucose-stimulated insulin secretion (GSIS) assay was carried out in vitro. Islets from all groups responded to low and high glucose and secreted more insulin at high glucose than at low glucose while maintaining their capability to shut down insulin secretion during a second low-glucose treatment (fig. S5B). The stimulation index (SI) (the ratio of insulin secretion at high glucose to that at low glucose) of islets cocultured with MSCs or eMSCs was significantly higher than that of islets cultured alone ($P < 0.05$) (Fig. 4C). This was likely caused by the beneficial paracrine effects between the MSCs and the islets (*32*–*36*).

Then, we investigated the persistence of MSC single cells and MSC spheroids in vivo. The GFP/luciferase MSCs were generated as reported previously (*5*). A total of 500 to 600 GFP/luciferase MSC spheroids (fig. S6A) and the corresponding number of GFP/luciferase MSC single cells were transplanted under the kidney capsule of healthy C57BL/6 mice. The whole-body images showed that no bioluminescent signals were detected after 14 days in mice receiving MSC single cells, while MSC spheroids survived as long as 30 days (fig. S6, B and C). Thus, MSC spheroids were chosen for the further experiments rather than MSC single-cell suspension because of the improved survival in vivo.

Next, we cotransplanted a marginal dose [150 to 200 islet equivalent (IEQ)] of syngeneic islets without MSCs (no-MSC group), with (500 to 600) MSC spheroids (MSC group), or with (500 to 600) eMSC spheroids (eMSC group) in the kidney capsule of streptozotocin (STZ)–induced C57BL/6 diabetic mice. The dosage of MSC spheroids was determined on the basis of the balance of having enough eMSCs to protect allogeneic islets while not occupying too much space and competing for oxygen and nutrients with islets. Non–fasting blood glucose curves showed that none of the mice in the no-MSC group and one of four mice in the MSC group became normoglycemic after transplantation (Fig. 4D). However, four of five mice reversed diabetes 4 days after transplantation in the eMSC group (Fig. 4D). The curve of diabetic mice percentage demonstrated that eMSCs significantly ($P < 0.05$) improved syngeneic islet engraftment with a median time to cure of 4 days and reduced islet number needed for diabetes correction (Fig. 4E). The intraperitoneal glucose tolerance test (IPGTT) performed on mice with different grafts on day 30 showed that four engrafted mice receiving islets with eMSCs and one engrafted mouse receiving islets with MSCs cleared blood glucose within 2 hours after injection (Fig. 4F); all other recipients failed to achieve metabolic control over glucose (Fig. 4F). The hematoxylin and eosin (H&E) and immunofluorescent staining showed the engraftment of islets cotransplanted with eMSCs in the kidney capsule and the expression of insulin and glucagon within the islets 30 days after transplantation (Fig. 4, G to I, and fig. S7). In contrast, islets without MSCs or with native MSCs were found to be less maintained in the kidney capsule as shown in the H&E staining (fig. S8). The improved outcome by the eMSCs may be due to their anti-inflammatory function, which will be discussed in more detail later.

PD-L1/CTLA4-Ig–overexpressing MSCs improve allogeneic islet transplantation

A more clinically relevant application of immunoprotective accessory cells such as the eMSCs would be for allogeneic transplantation. We therefore cotransplanted BALB/c mouse islets with eMSCs into diabetic C57BL/6 mice to test whether they could delay allorejection. Islets transplanted without MSCs (no-MSC group) or with native MSCs (MSC group) were included as control. In each mouse, around 500 to 600 IEQ BALB/c mouse islets were transplanted in one of the kidney capsules (Fig. 5A). The blood glucose curves showed that BALB/c islets in the no-MSC group or MSC group were all rejected within 14 and 20 days, respectively (Fig. 5, B and C). In contrast, mice transplanted with islets and 500 to 600 eMSC spheroids maintained normoglycemia for as long as 100 days (Fig. 5, B and C). Quantitative analysis showed that allogeneic islets cotransplanted with eMSCs survived significantly longer than the other two groups ($P < 0.0001$) (Fig. 5C). The median survival times of these three groups were 14 days (no MSC), 14 days (MSC), and 40 days (eMSC) ($n = 9$), indicating that the eMSCs significantly delayed allorejection and prolonged allograft survival compared to other groups ($P < 0.0001$) (Fig. 5, B and C). The IPGTT performed on mice with different grafts on day 30 showed that mice receiving islets with eMSCs cleared blood glucose within 2 hours after injection, similar to the healthy mice, while those receiving islets without MSCs or with MSCs failed to achieve metabolic control over glucose (Fig. 5D and fig. S9).

To continuously and more directly monitor islet survival in vivo, around 500 IEQ GFP/luciferase expressing friend virus B (FVB) mouse islets were transplanted in the kidney capsule of diabetic C57BL/6 mice. The bioluminescent imaging showed that the signal was localized in the kidney, and allogeneic islets without MSCs were rejected within 14 days (Fig. 5E). Although better islet survival was observed within 7 days when islets were cotransplanted with MSCs compared to the no-MSC group, the islets were eventually rejected within 14 days (Fig. 5, E and F). However, the bioluminescent signal lasted for as long as 70 days when islets were cotransplanted with the eMSCs, and they were not completely rejected until day 84 (Fig. 5, E and F). Quantitative analysis confirmed that the eMSCs significantly improved allogeneic islet survival compared to no-MSC and MSC groups ($P < 0.001$) (Fig. 5, F and G).

We then asked the question whether the immunomodulatory effects of the eMSCs are only local and not systemic. To answer this question, we investigated the systemic immune response in the

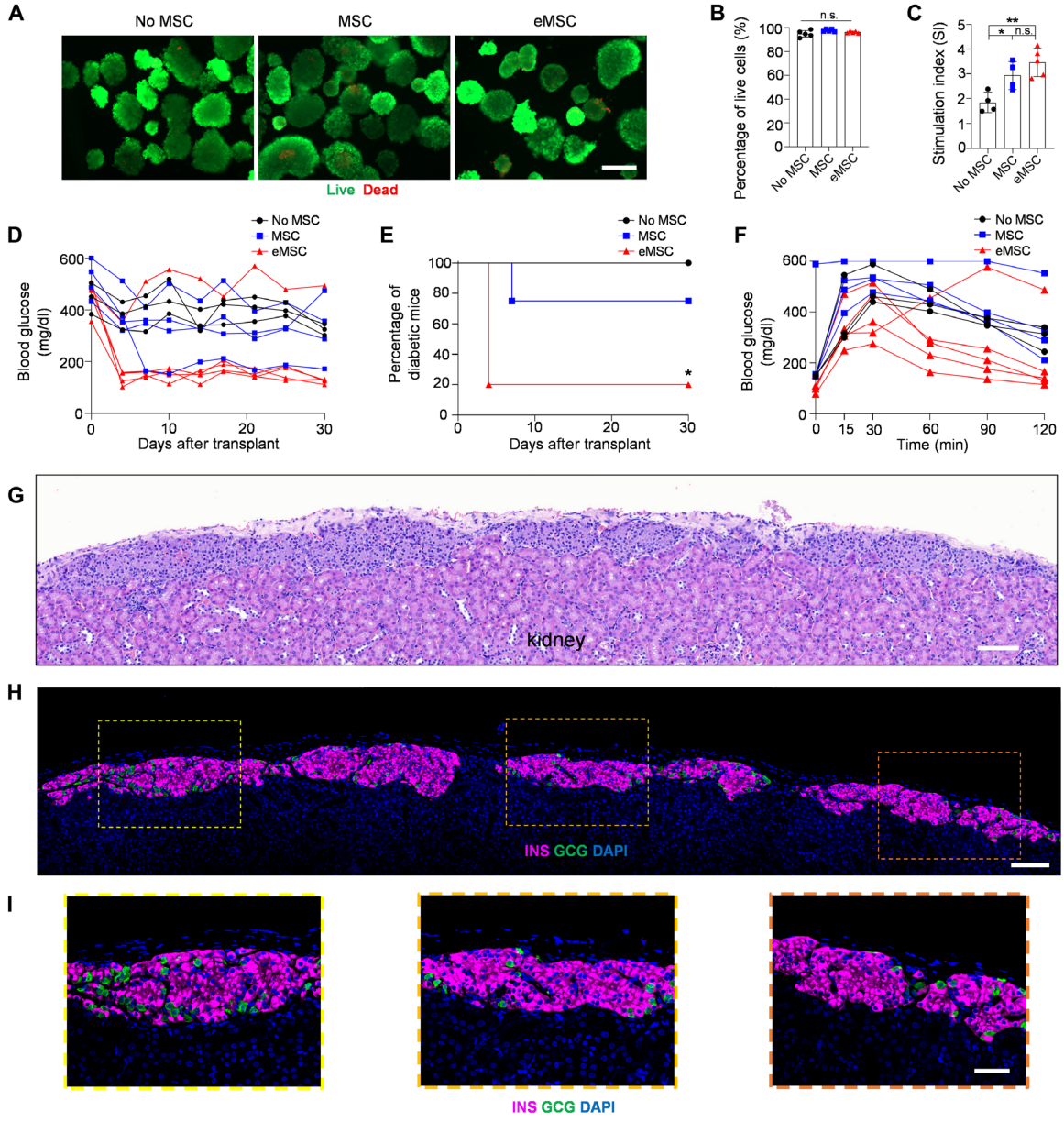

Fig. 4. PD-L1/CTLA4-Ig–overexpressing eMSCs improve syngeneic islet transplantation in mice. (**A**) Live and dead staining of islets cocultured without MSCs, with MSC spheroids, or with eMSC spheroids in vitro for 24 hours (green, live cells; red, dead cells). (**B**) Quantitative analysis of fluorescence intensity of images shown in (A) ($n = 5$). (**C**) Stimulation index of islets (the ratio of insulin secretion at high glucose to that at low glucose) cocultured without MSCs, with MSC spheroids, or with eMSC spheroids for 24 hours ($n = 4$ to 5). (**D**) Blood glucose curves of diabetic C57BL/6 mice transplanted with syngeneic islets with a marginal dosage without MSCs (no-MSC group) ($n = 3$), with MSC spheroids (MSC group) ($n = 4$), and with eMSC spheroids (eMSC group) ($n = 5$) in the kidney capsule. (**E**) Graft survival curves of indicated groups shown in (D). (**F**) Blood glucose measurement in the intraperitoneal glucose tolerance test of different groups ($n = 3$ to 5). (**G**) Representative H&E staining of syngeneic islets with eMSC engrafted in diabetic C57BL/6 mice in the kidney capsule. (**H**) Representative immunofluorescent staining of syngeneic islets with eMSCs engrafted in diabetic C57BL/6 mice in the kidney capsule. DAPI (gray), insulin (INS, magenta), and glucagon (GCG, green). (**I**) Higher magnification of islets in (H). One-way ANOVA followed by Tukey's test was performed for comparing the multigroup data. Survival curve was analyzed using a Mantel-Cox test. The level of significance was labeled by n.s., *, and **, denoting nonsignificant and P values of <0.05 and <0.01, respectively. Scale bars, 50 μm (A and I) and 100 μm (G and H).

spleen of diabetic C57BL/6 mice receiving allogeneic islets with/without MSCs or with eMSCs on day 14 after transplantation. The data suggested that $CD3^+$ T cells and PD-1^+ cells were observed in the spleen in all three groups with an average density of 10,000 and 15,000 cells/mm^2, respectively (fig. S10). There was no difference among the three groups in terms of the $CD3^+$ T cell and PD-1^+ cell densities ($P > 0.05$) (fig. S10, B and C). Besides this, we transplanted ~500 to 600 IEQ BALB/c islets and 500 to 600 eMSC spheroids separately into two kidneys in the same C57BL/6 mouse recipient with diabetes (fig. S11A). The blood glucose curves showed that islets were rejected in all the recipients within 14 days, and the eMSCs did not have any protective effects on allogeneic islets that were

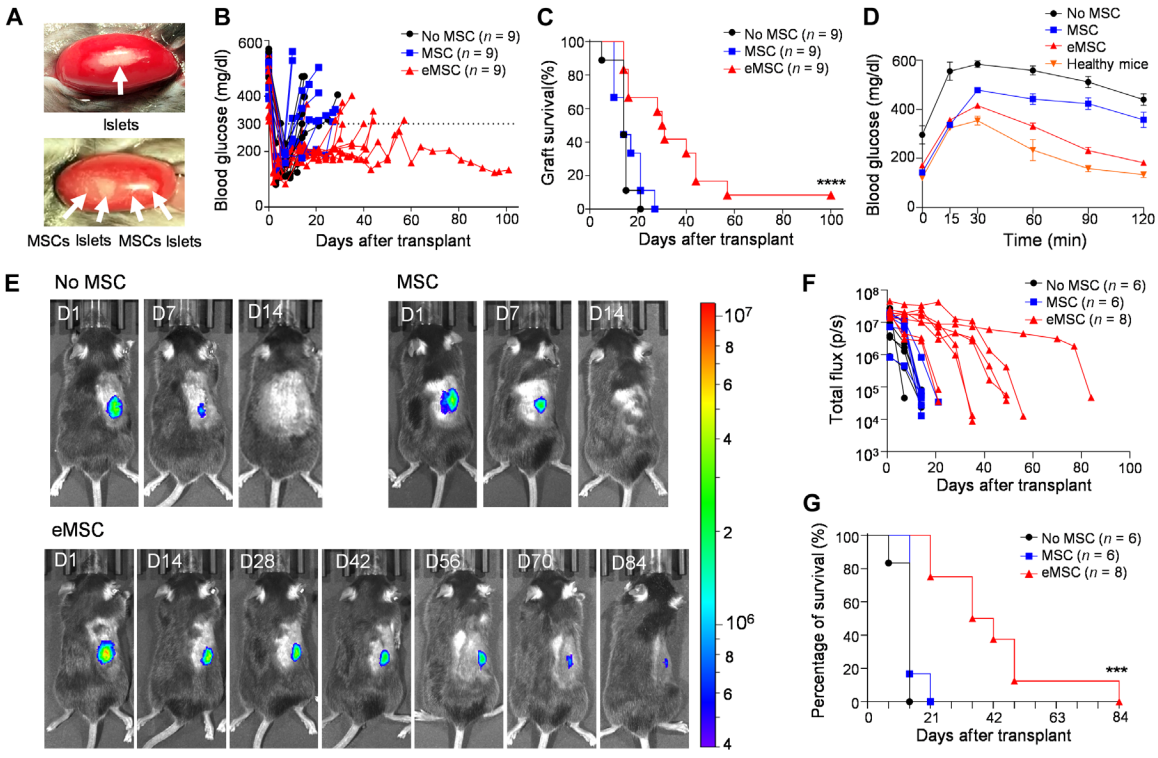

Fig. 5. PD-L1/CTLA4-Ig–overexpressing eMSCs delay allogeneic islet rejection in mice. (**A**) Representative digital images of kidneys transplanted with islets alone (top) or with either MSC or eMSC spheroids (bottom). (**B**) Blood glucose curves of diabetic C57BL/6 mice transplanted with BALB/c islets without MSCs (no-MSC group) ($n = 9$), BALB/c islets with MSC spheroids (MSC group) ($n = 9$), and BALB/c islets with eMSC spheroids (eMSC group) ($n = 9$) in the kidney capsule. (**C**) Graft survival curve of indicated groups shown in (B). (**D**) Blood glucose measurement in the intraperitoneal glucose tolerance test of different groups ($n = 3$). (**E**) Bioluminescent images of diabetic C57BL/6 mice transplanted with GFP/luciferase FVB mouse islets without MSCs (no-MSC group) ($n = 6$), with MSC spheroids (MSC group) ($n = 6$), or with eMSC spheroids (eMSC group) ($n = 8$) in the kidney capsule. (**F**) Quantitative analysis of bioluminescent signals measured in mice with different grafts ($n = 6$ to 8). (**G**) Graft survival curve of indicated groups in (F) ($n = 6$ to 8). Survival curve was analyzed using a Mantel-Cox test. The level of significance was labeled by *** and ****, denoting *P* values of <0.001 and <0.0001, respectively.

transplanted in different kidney capsules (fig. S11B). Together, the data suggest that the immunomodulation by the eMSCs is a local effect (figs. S10 and S11).

PD-L1/CTLA4-Ig–overexpressing MSCs promote immune tolerant microenvironment

To understand how the eMSCs protected the islets from allorejection, we first examined the progression of immune response in allogeneic islet grafts with no MSCs. Grafts were retrieved on days 5, 8, and 15 and analyzed by H&E and immunofluorescent staining. Histological images demonstrated that host immune cells infiltrated the allograft on day 5, accumulated around the islets on day 8, and, lastly, replaced islet cells on day 15 (fig. S12). Immunofluorescent staining images of grafts showed that insulin$^+$ β cells were surrounded and infiltrated by host CD3$^+$ T cells (fig. S13, A and B). The ratio of CD3$^+$ T cells to insulin$^+$ β cells in allograft retrieved on day 8 was significantly higher than that on day 5 ($P < 0.01$), indicating progressive T cell infiltration over time (fig. S13, A to C). Costaining of CD3 with CD4 or CD3 with CD8 demonstrated that the infiltrated T cells were CD4$^+$ or CD8$^+$ T cells (fig. S13, D to I) and both types of cells increased in number significantly from day 5 to day 8 ($P < 0.05$), a time point we chose for the immune profiling in all the groups.

We next characterized the immune cells at the graft site in response to the PD-L1/CTLA4-Ig presentation by transplanting allogeneic islets (500 IEQ) without any MSCs or with either MSCs or eMSCs into diabetic C57BL/6 mice. On day 8 after transplantation, the grafts were explanted and the cells within the graft tissues were isolated. Flow cytometry analysis was carried out to identify the immune cell population based on the expression of markers including CD45, CD3, CD4, CD8, CD25, CD44, CD62L, CD11c, CD86, Foxp3, and PD-1 (fig. S14). Results showed that the percentage of CD3$^+$ T cells in eMSC grafts was significantly lower than those in no-MSC grafts and MSC grafts ($P < 0.01$) (Fig. 6A). Although there was no difference in terms of the CD4$^+$ T cell percentage in CD45$^+$ cell population among different groups ($P > 0.05$), the CD8$^+$ T cells in the CD45$^+$ cell population were significantly fewer in the eMSC group compared to the other two groups ($P < 0.01$) (fig. S15, A and B). In addition, more CD4$^+$ T cells and fewer CD8$^+$ T cells were observed within the CD3$^+$ T cell population in the eMSC group compared to the other two groups ($P < 0.05$) (fig. S15, C and D). Furthermore, the percentage of CD4$^+$ and CD8$^+$ T_{eff} cells (CD44^{hi}CD62L^{lo}) and activated dendritic cells (CD11c$^+$CD86$^+$) also decreased significantly in eMSC grafts compared to the other groups ($P < 0.05$) (Fig. 6, B to D). It was additionally found that the percentage of CD8$^+$ T cells expressing an exhaustion/anergy marker such as PD-1 increased significantly in the eMSC group compared to the no-MSC group ($P < 0.01$) (Fig. 6E). Further investigation revealed that the percentage of CD4$^+$ T_{reg} cells (CD4$^+$CD25$^+$Foxp3$^+$)

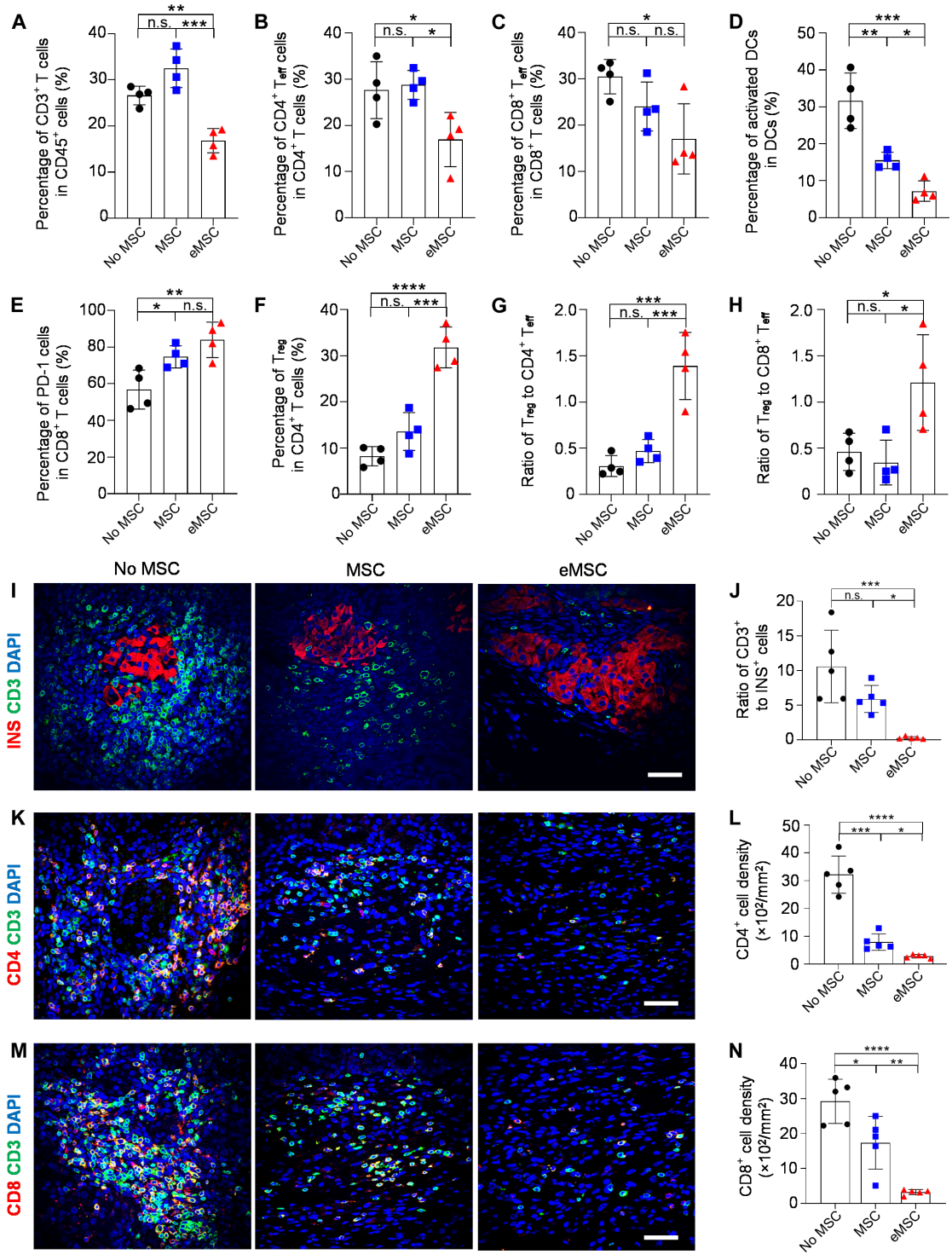

Fig. 6. Characterization of immune cells in the local microenvironment of the islet allografts in mice. (**A**) Percentage of $CD3^+$ T cells in $CD45^+$ cells ($n = 4$). (**B**) Percentage of $CD4^+$ T_{eff} cells in $CD4^+$ T cells ($n = 4$). (**C**) Percentage of $CD8^+$ T_{eff} cells in $CD8^+$ T cells ($n = 4$). (**D**) Percentage of activated dendritic cells (DCs) in DCs ($n = 4$). (**E**) Percentage of PD-1^+ cells in $CD8^+$ T cells ($n = 4$). (**F**) Percentage of T_{reg} cells in $CD4^+$ T cells ($n = 4$). (**G**) Ratio of T_{reg} to $CD4^+$ T_{eff} cells ($n = 4$). (**H**) Ratio of T_{reg} cells to $CD8^+$ T_{eff} cells ($n = 4$). (**I**) Representative immunofluorescent staining of islet grafts (DAPI, blue; INS, red; CD3, green). (**J**) Ratio of $CD3^+$ T cells to insulin$^+$ β cells shown in (I) ($n = 5$). (**K**) Representative immunofluorescent staining of islet grafts (DAPI, blue; CD4. red; CD3, green). (**L**) Quantitative analysis of $CD4^+$ T cell density shown in (K) ($n = 5$). (**M**) Representative immunofluorescent staining of islet grafts (DAPI, blue; CD8, red; CD3, green). (**N**) Quantitative analysis of $CD8^+$ T cell density shown in (M) ($n = 5$). One-way ANOVA followed by Tukey's test was performed for comparing the multigroup data. The level of significance was labeled by n.s., *, **, ***, and ****, denoting nonsignificant and P values of <0.05, <0.01, <0.001, and <0.0001, respectively. Scale bars, 50 μm (I, K, and M).

(Fig. 6F) and the ratio of $CD4^+$ T_{reg} cells to $CD4^+$ or $CD8^+$ T_{eff} cells (Fig. 6, G and H) in the eMSC group were significantly higher than those in the other two groups ($P < 0.05$).

Histological analysis of different grafts retrieved on day 8 corroborated the trends observed from flow cytometry. Specifically, immunofluorescent staining showed that the density of $CD3^+$ T cells and the ratio of $CD3^+$ T cells to insulin$^+$ β cells decreased significantly in allografts cotransplanted with eMSCs than those without MSCs or with MSCs ($P < 0.05$) (Fig. 6, I and J). The densities of $CD4^+$ and $CD8^+$ T cells in the grafts cotransplanted with eMSCs were also significantly lower than those in the other two groups ($P < 0.05$) (Fig. 6, K to N).

We further analyzed the grafts after a longer-term transplantation. The H&E image showed that allogeneic islets were maintained in the kidney capsule after 45 days' transplantation (Fig. 7A). Immunofluorescent staining for insulin and glucagon demonstrated that cells maintained their individual hormone identities, and many insulin-expressing β cells survived in the allogeneic mice (Fig. 7B). Costaining of insulin and Foxp3 showed that insulin$^+$ β cells were surrounded by many $Foxp3^+$ T_{reg} cells (Fig. 7, C and D, and fig. S16), which might be responsible for the long-term survival of allogeneic islets in vivo. The $Foxp3^+$ T_{reg} cells within the grafts were further confirmed to express CD4 marker by costaining of CD4 and Foxp3 (Fig. 7E and fig. S16). Furthermore, examination of the retrieved grafts 103 days after transplantation showed the survival of insulin$^+$ β cells surrounded by $CD4^+Foxp3^+$ T_{reg} cells (Fig. 7F and fig. S16). Quantitative analysis showed that the density of $Foxp3^+$ T_{reg} cells in the eMSC graft in the long term was around 450/mm^2, while there was no $Foxp3^+$ T_{reg} cells found in the eradicated allograft in the other two groups (Fig. 7G). The percentage of $Foxp3^+$ T_{reg} cells in the $CD4^+$ T cells was around 60% within the eMSC graft, which was significantly higher than that in no-MSC and MSC grafts ($P < 0.0001$) (Fig. 7H). Together, these data showed that the eMSCs suppressed $CD4^+$ and $CD8^+$ T_{eff} cells and promoted $CD4^+$ T_{reg} cells within the graft. This tolerant immune microenvironment may be responsible for the delayed allorejection and prolonged islet survival.

DISCUSSION

Islet transplantation offers T1D patients many benefits including improved glucose control, prevention of dangerous hypoglycemia unawareness, and reduced risks of diabetes-related complications. However, chronic systemic immunosuppression required to prevent immune rejection can affect the longevity of the implanted islets and trigger adverse side effects on patients such as infections and cancer. In this study, we set out to develop a type of immunoprotective accessory cells that can be mixed and cotransplanted with islets using established clinical procedures but with no or reduced systemic immunosuppression.

We chose MSCs as the starting cells for multiple reasons. They exist in many tissues, can be obtained by isolating fat tissues with minimally invasive surgery, have been widely used in clinical applications for tissue regeneration, and have an acceptable safety profile (*31*, *37*). To date, more than 1000 clinical trials exploring MSCs are registered by the U.S. Food and Drug Administration and many have demonstrated that MSCs can be safely infused even in high doses in patients (*38*, *39*). For example, in a phase 1/2 trial (TREAT-ME1, NCT02008539), which involved intravenous administration of autologous MSCs engineered to express the tumor-specific herpes simplex virus–thymidine kinase gene to treat gastrointestinal tumors, investigators reported favorable safety in patients who received the treatment (*40*). Previous studies have also shown that MSCs infused with islets into the hepatic portal vein improved syngeneic rat islet (*34*) engraftment in rat and human islet (*41*) engraftment in immunodeficient mice and promoted vascularization by secreting paracrine factors (*31*, *34*, *36*, *37*, *41*). To create the eMSCs with immunoprotective function, we expressed PD-L1 on their surface and CTLA4-Ig as an extracellularly released factor. PD-1 (CD279) and CTLA-4 (CD152) are two critical and potent regulators of peripheral T cell tolerance and T cell function (*42*, *43*); these two signaling pathways have been used in modulating alloreactive responses in multiple transplantation models. Engineering of primary islets with PD-L1 and/or CTLA4-Ig by gene modification or protein conjugation resulted in survival of islet allograft for more than 100 days (*29*, *30*). Knocking in human PD-L1 and CTLA4-Ig to human embryonic stem cells protected them from allogeneic immune responses in humanized mice (*44*). Overexpression of PD-L1 protected stem cell–derived islet organoids in diabetic xenogeneic mice and allogeneic humanized mice and restored glucose homeostasis for 50 and 25 days, respectively (*45*). Despite these advances, manipulation of islets can be laborious and negatively affect their function, and generation of hypoimmunogenic cells from stem cells may cause safety concerns (*46*). Therefore, accessory cells such as the eMSCs we created in this study may provide an easier and safer way to circumvent the need for chronic systemic immunosuppression in islet transplantation.

The eMSCs had similar gene expressions to the MSCs except for the exogenous PD-L1/CTLA4-Ig genes that were purposely introduced and had overexpression by hundred-fold. We used MSC spheroids to cotransplant with islets instead of using single cells because MSC spheroids showed improved survival compared to MSC single cells in kidney capsule. In addition, previous studies showed elevated gene expressions associated with anti-apoptotic factors such as B cell lymphoma extra large (Bcl-xL) and proangiogenesis factors such as vascular endothelial growth factor, fibroblast growth factor-2, and hepatocyte growth factor in spheroids compared to the cells in the two-dimensional monolayer culture (*47*, *48*). Both the MSC or eMSC spheroids were compatible with islets in vitro and improved their glucose-stimulated insulin secretion after coculture with islets. Furthermore, the eMSCs were shown to be able to suppress T cell proliferation, activation, and cytotoxicity of allogeneic and diabetogenic $CD4^+$ and $CD8^+$ in vitro in a mixed lymphocyte reaction in the presence of allogeneic antigen-presenting cells. The in vitro results suggested that eMSCs could not only protect islets immunologically by inhibiting T_{eff} cells but also enhance their function by paracrine factors.

The therapeutic potential of the eMSCs was first demonstrated in a syngeneic islet transplantation model. Autologous islet transplantation is a clinically proven treatment option for patients with chronic pancreatitis who undergo pancreatectomy. However, even in the absence of immune rejection, the early posttransplant inflammation can cause extensive β cell loss (*49*, *50*). Therefore, inhibition of early inflammatory events is expected to improve long-term islet function. The signaling pathway of PD-L1 and CTLA4 can regulate not only alloresponses but also inflammatory responses. The up-regulation of PD-L1 expression in response to inflammatory cytokines acts as a natural "balance" to limit tissue-specific

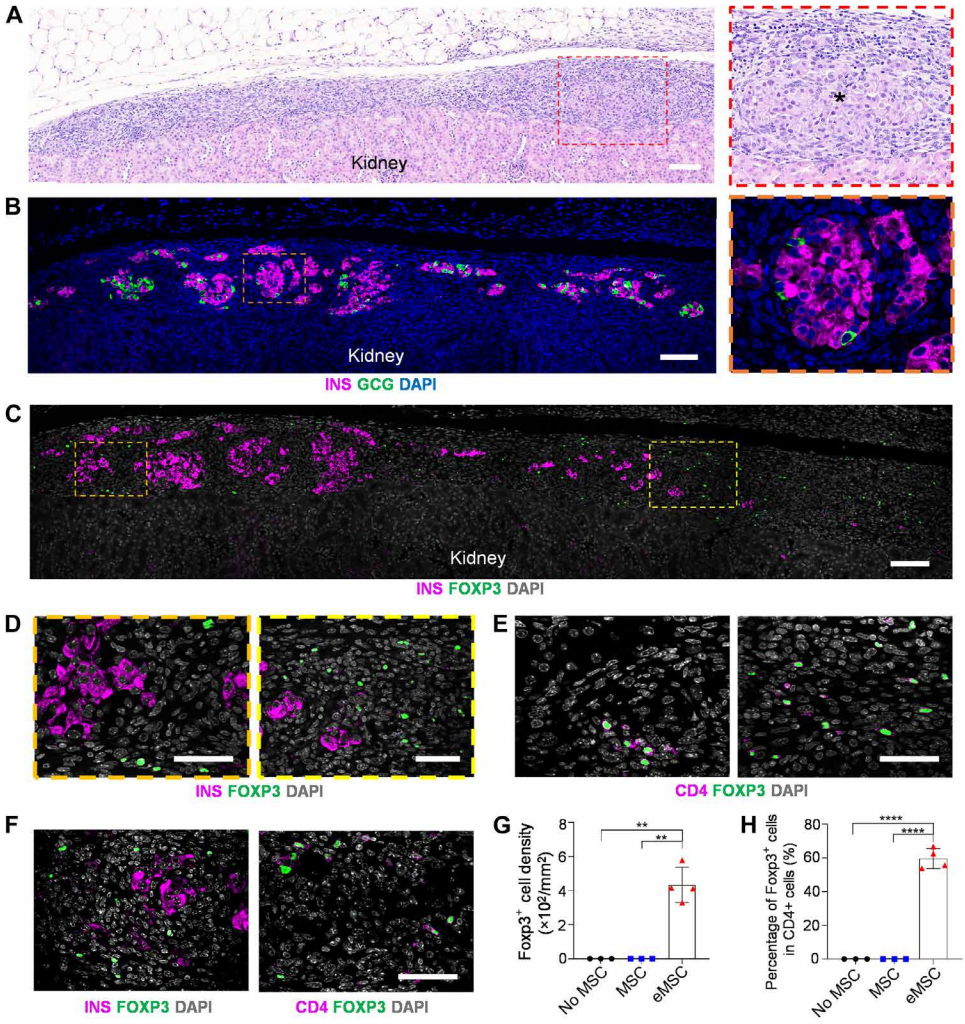

Fig. 7. Ex vivo characterization of allografts with eMSCs. (**A**) Representative H&E image of islet grafts with eMSCs explanted on day 45 (higher-magnification image on the right). The asterisk indicates the allogeneic islet. (**B**) Representative immunofluorescent staining of islet grafts with eMSCs explanted on day 45 with markers DAPI (gray), insulin (INS, magenta), and glucagon (GCG, green) (higher-magnification image on the right). (**C**) Representative immunofluorescent staining of islet grafts with eMSCs explanted on day 45 with markers DAPI (gray), insulin (INS, magenta), and Foxp3 (green). (**D**) Higher-magnification images from (C). (**E**) Representative immunofluorescent staining of islet grafts with eMSCs explanted on day 45 with markers DAPI (gray), CD4 (magenta), and Foxp3 (green). (**F**) Representative immunofluorescent staining of islet grafts with eMSCs explanted on day 103. Left: DAPI (gray), insulin (INS, magenta), and Foxp3 (green). Right: DAPI (gray), CD4 (magenta), and Foxp3 (green). (**G**) Foxp3$^+$ T_{reg} cell density within the islet grafts [$n = 3$ for no-MSC and MSC groups (grafts retrieved on day 30) and $n = 4$ for eMSC group (grafts retrieved between 45 and 103 days)]. (**H**) Percentage of Foxp3$^+$ T_{reg} cells in the CD4$^+$ T cell population within the retrieved grafts [$n = 3$ for no-MSC and MSC groups (grafts retrieved on day 30) and $n = 4$ for the eMSC group (grafts retrieved between 45 and 103 days)]. One-way ANOVA followed by Tukey's test was performed for comparing the multigroup data. The level of significance was labeled by ** and ****, denoting P values of <0.01 and <0.0001, respectively. Scale bars, 50 μm (D to F) and 100 μm (A to C).

responses to inflammation (*51*, *52*). For example, genetically modified PD-L1–overexpressing dendritic cells differentiated from mouse embryonic stem (ES) cells were demonstrated to limit spinal cord inflammation (*53*). Similarly, CTLA-4 signaling also helps bring an inflammatory response back down to homeostatic levels (*42*). For example, CTLA4-Ig therapy can reduce joint inflammation and damage in patients with active rheumatoid arthritis, which is a systemic inflammatory disorder (*54*). Thus, the observed improvement of syngeneic islet transplantation using eMSCs with PD-L1 and CTLA4-Ig expression might be explained by the anti-inflammatory properties of these two ligands. The eMSCs may offer a new option to mitigate the early inflammation and improve autologous islet transplantation.

The eMSCs were also shown to improve the allogeneic islet transplantation in a diabetic mouse model. Without any immunosuppression, the eMSCs delayed allograft failure significantly, as evidenced by both blood glucose monitoring and bioluminescent imaging. Although the kidney capsule transplantation used in this study is different from the portal vein transplantation in clinical practice, it is possible that the eMSCs may be mixed with islets and cotransplanted into the portal vein (*41*, *55*). Therefore, future studies may be directed at testing whether eMSCs can be used in portal vein and eventually clinical islet transplantation and improve the therapeutic outcome with reduced systemic immunosuppression. We analyzed local immune responses in the eMSC/islet graft at different time points

using flow cytometry and immunostaining. The results showed the eMSCs suppressed host $CD4^+$ and $CD8^+$ T_{eff} cell activation, induced T cell exhaustion, and promoted T_{reg} cells, all of which could be responsible for the observed delay of allorejection.

Pioneering work has been done recently on synthetic biomaterial platforms for local immunomodulation for islet transplantation. For example, PEG microgels or poly(lactide-co-glycolide) (PLG) scaffold were modified to display PD-L1 and Fas ligand (FasL) through a streptavidin/biotin interaction (*27*, *56*, *57*). Long-term (>100 days) survival of allogeneic islets was achieved using biomaterial approaches combined with a short course of rapamycin treatment. Synthetic biomaterials allow islet transplantation at extrahepatic sites such as omentum, but they can cause foreign body responses, induce antibodies, and may be challenging to be used in current clinical protocol, i.e., portal vein transplantation. In contrast, accessory cells such as the eMSCs can be obtained from autologous source, secrete a wide spectrum of beneficial paracrine factors, and be mixed with islets and transplanted with no or minimal modifications of current clinical procedures. In addition, factors delivered or presented by biomaterials may be depleted or degraded over time. The accessory cells on the other hand act as a "living factory" to produce tolerogenic ligands, either immobilized on the cell surface or released to the local environment. The eMSCs enabled the allogenic islet survival for up to more than 100 days with no short-term treatment of rapamycin or other immunosuppressive drugs.

T_{reg} cells have been shown to play an important role in maintaining homeostasis and peripheral tolerance (*58*, *59*). Both systemic infusion of autologous T_{reg} cells (*60*, *61*) and cotransplantation of T_{reg} with islets (*62*, *63*) have been investigated in treating diabetes and shown therapeutic effects in preclinical trials. However, the mass production of T_{reg} cells and the maintenance of their long-term function remain challenging. Thus, there are attempts to engineer other cell types with regulatory ligands. In one study, syngeneic myoblasts were edited to express FasL on the cell surface and protected islet allograft (*64*). However, myoblasts are relatively difficult to acquire noninvasively. In addition, while FasL induces T cell death (*65*), it may also activate innate immune responses (*66*). In another study, researchers engineered syngeneic fibroblasts using adenovirus to overexpress indoleamine 2,3 dioxygenase (IDO) and achieved allograft survival in IDO-expressing composite up to 51 days (*67*). Although IDO degrades tryptophan required for T cell growth and suppresses T cell responses (*68*, *69*), the potency of IDO pathway may be lower compared to PD-L1 (*70*, *71*). Nevertheless, CTLA4-Ig has been reported to trigger the production of IDO in APCs (*23*), suggesting multiple ways in which immune regulation following CTLA4-Ig treatment may occur. Furthermore, in both studies, the immunomodulatory ligands were either immobilized on the cell surface or released to the peripheral environment. In the eMSCs we described here, the PD-L1 was immobilized on the cell surface and CTLA4-Ig was released. This dual modulation approach suppresses T cell function in a nonredundant way (*24*, *25*).

Limitations exist in this study. For example, although the eMSCs significantly improved islet survival in allogeneic diabetic mice without any immunosuppression, long-term engraftment in many of the recipients was not achieved. The different outcomes among the recipients might be caused mainly by the lack of MSC persistence in vivo, which resulted in the graft failure and eventual allograft rejection. Previous studies also observed insufficient survival of MSCs at the site of administration, which might be attributed to multiple issues such as apoptosis, hypoxia, and inflammation (*38*, *72*–*74*). Bioengineering strategies such as priming MSCs with hypoxia, inflammatory cytokines and small molecules have been investigated and shown to improve the survival of MSCs (*38*, *75*, *76*). Together, it was highlighted that the survival of MSCs following local administration needs to be enhanced to improve the therapeutic outcome. There are other factors causing the variation including intrinsic biological variation and unintentional inconsistencies such as cell numbers, spatial distributions, and surgeries. For example, it was challenging to achieve homogeneous dispersion of MSCs and islets when they were delivered to the mouse kidney capsule. While T_{reg} cells surrounding the allograft could modulate the immune responses, some islets could still be exposed to the T_{eff} cells and the gradual T cell infiltration in the long-term would eventually result in destruction of the islets. Better preparation and surgical techniques may improve the therapeutic outcome. Another limitation is that the acquisition and modification of autologous MSCs would be time-consuming, compared to other strategies using off-the-shelf products such as synthetic biomaterial platforms or universal stem cell–derived β cells. Further investigation will be needed to test whether allogeneic modified MSCs have the potential to achieve the same therapeutic effects as autologous modified MSCs. Last, all the experiments described in this study were performed in mice using kidney capsule transplantation without considering autoimmune responses. Although the function of eMSCs in protecting allogeneic islets was not investigated in NOD mice in this study, we showed decreased proliferation, activation, and cytotoxicity of diabetogenic T cells in the in vitro T cell proliferation and activation studies that were carried out using splenocytes isolated from transgenic NOD mice, which might guide the in vivo studies in the future. In addition, future studies should be directed at portal vein transplantation to test whether the eMSCs may be used in clinical islet transplantation to improve graft function and therapeutic outcome with reduced and minimal systemic immunosuppression.

MATERIALS AND METHODS

Experimental design

The purpose of this study was to develop a type of immunoprotective accessory cells that can protect allogeneic islets with no or reduced systemic immunosuppression. Animals were handled and cared for by trained scientists and approved by the Cornell Institutional Animal Care and Use Committee. Sample size, including number of mice per group, was chosen to ensure adequate power and was based on historical data. All mice used were males to eliminate any potential confounding influences of gender differences. All mice were randomly assigned to treatment groups, and all data collection and analyses were performed blindly for different treatment conditions. The number of biologic replicates is specified in the figure legends.

Animals

Eight-week-old male C57BL/6, BALB/c, and FVB-Tg(CAG-luc,-GFP)L2G85Chco/J (L2G85) mice were purchased from the Jackson Laboratory (Bar Harbor, ME). All animal procedures were approved by the Cornell Institutional Animal Care and Use Committee.

Cell culture

Strain C57BL/6 mouse MSCs (Cyagen, MUBMX-01001) were purchased. The 293T cell line and the 4T1 cell line were received as

gifts. 293T cells were cultured in Dulbecco's modified Eagle's medium (Gibco, 2051526) supplemented with 10% FBS and 1% penicillin/streptomycin (P/S). 4T1 cells were cultured in RPMI 1640 media with 10% FBS and 1% P/S. MSCs were cultured in MSC growth medium (Cyagen, GUXMX-90011) following the manufacturer's instruction. Primary islets were cultured in RPMI 1640 media with 10% FBS and 1% P/S. Splenocytes were cultured in RPMI 1640 media (Thermo Fisher Scientific, 11875093) with 5% FBS, 1% P/S, 1% L-glutamine (Thermo Fisher Scientific, 25030149), and 0.1% 2-mercaptoethanol (Thermo Fisher Scientific, 31350010).

Generation of GFP/luciferase-expressing cell line

Plasmid containing enhanced GFP gene [720 base pairs (bp)] and humanized firefly luciferase (Luc2) gene (1653 bp) was constructed by Vector Builder. GFP^+/$luciferase^+$ 4T1 cells and GFP^+/$luciferase^+$ MSCs were generated following a previous publication (*5*) and verified under a fluorescence microscope.

Generation of PD-L1 and CTLA4-Ig–expressing cell lines

The pLenti-based expression vector containing mouse PD-L1 gene (873 bp) and CTLA4-Ig gene (1179 bp) was constructed by Vector Builder. 293T cells were plated and cultured in 10-cm treated tissue culture plate the day before transduction to obtain 90 to 95% confluency. The lentiviral stocks were produced by transfecting 293T cells with the designed vector using the ViraPower Bsd Lentiviral Support Kit (Thermo Fisher Scientific, K497000) following the manufacturer's instruction. After 48 to 72 hours after transfection, the lentiviral supernatant was collected, centrifuged at 3000 rpm for 15 min at 4°C to pellet debris, and stored at −80°C. MSC single cells were prepared and seeded in a six-well plate (5000 cells per well) with 2 ml of virus-containing supernatant. After 48 hours of transduction, lentivirus medium was discarded, and fresh MSC culture medium was added. Bsd solution with a final concentration of 5 μg/ml was used to purify the transfected cells. The PD-L1/CTLA4-Ig GFP/luciferase 4T1 cells were generated in the same manner as PD-L1/CTLA4-Ig MSCs. For the formation of MSC spheroids, about 4 ml of solution containing 4 million MSCs was added in one well of six-well suspension culture plate (Genesee Scientific, 25-100). Then, the cells were cultured on an orbital shaker with a speed of 100 rpm overnight. The spheroids were collected and centrifuged into cell pellet for further use.

Quantitative reverse transcription PCR

Five million MSCs or eMSCs were collected in the tube and centrifuged into a cell pellet. Total RNA of two groups was isolated with an RNeasy kit (Qiagen, 74106), and complementary DNA was prepared using reverse transcriptase III (Thermo Fisher Scientific, 4368814), according to the manufacturer's instruction. Quantitative PCR was performed using SYBR Green Master Mix (Thermo Fisher Scientific, A25776), and detection was achieved using the StepOnePlus Real-time PCR system thermocycler (Applied Biosystems). Expression of target genes was normalized to glyceraldehyde-3-phosphate dehydrogenase (GAPDH). Real-time PCR primer sequences are listed in table S1.

Western blot

Five million MSCs or eMSCs were collected in the tube and centrifuged into a cell pellet. Cells were lysed with radioimmunoprecipitation assay lysis buffer (Thermo Fisher Scientific, 89901) in the presence of protease inhibitor. The concentration of extracted protein was measured using Pierce 660-nm protein assay reagent (Thermo Fisher Scientific, 1861426) and the Bio-Rad SmartSpec 3000 spectrophotometer. Forty micrograms of whole-cell protein lysate was applied to 4 to 15% Mini-PROTEAN TGX precast protein gel (Bio-Rad, 4561084) with electrophoresis and then transferred to a nitrocellulose membrane. The probed primary antibodies were detected by using horseradish peroxidase–conjugated secondary antibodies and the enhanced chemiluminescent detection system (GE Healthcare, 28906836). Primary and secondary antibodies are detailed in table S2.

Enzyme-linked immunosorbent assay

One million MSCs or eMSCs were seeded in one well of a 12-well culture plate with 1 ml of culture medium in each well. Cells were cultured for 6 hours in an incubator. Culture media were collected in tubes, and the supernatant was collected after centrifuge. The CTLA4-Ig in the supernatant was quantified by Mouse CTLA-4 DuoSet ELISA (R&D Systems, DY476) according to the manufacturer's instruction. Absorbance of reaction solution at 450 nm was measured in the Synergy plate reader (Biotek).

Flow cytometry

For analysis of MSCs and 4T1 cells before and after modification, the cells were detached from the culture dish by using TrypLE, centrifuged, and washed with PBS. The cells were blocked with staining buffer, incubated for 15 min at 4°C with antibodies (table S3), washed with staining buffer, and resuspended in staining buffer to analyze on an Attune NxT flow cytometer (Thermo Fisher Scientific). Native 4T1 cells engrafted in BALB/c mice and modified 4T1 cells engrafted in C57BL/6 mice were dissociated into single cells with mechanical force. The cells were filtered through a 40-μm strainer (VWR, 10199-654). The single cells were then stained with antibody (APC anti-mouse PD-L1 antibody, BioLegend, 124311) and analyzed following the steps as described above. The data were analyzed and generated by FlowJo software v10.7.

Immunofluorescent staining

Cells were seeded in eight-well Lab-Tek chamber slides at a density of 50,000 cells/cm^2. After confluency, cells were fixed in 10% formalin and then blocked for 30 min in 5% donkey serum (Sigma-Aldrich, S30-M). Subsequently, cells were incubated with primary antibodies (rabbit anti-mouse PD-L1 antibody, R&D Systems, MAB90781-SP) for 30 min at room temperature. Cells were washed three times with PBS and then incubated with secondary antibodies [donkey anti-rabbit immunoglobulin G (H + L) highly cross-adsorbed secondary antibody, Alexa Fluor 488, Thermo Fisher Scientific, A21206] for 30 min at room temperature. Cells were washed three times with PBS and stained with 4′,6-diamidino-2-phenylindole (DAPI) (0.5 μg/ml) for 5 min. Slides were mounted with fluorescence mounting medium (Sigma-Aldrich, F6057). Slides were imaged using confocal microscopy (FV1000, Olympus, Japan).

In vitro T cell suppression assay

MSCs or eMSCs were seeded at a density of 20,000 per well in a U-bottom 96-well plate and incubated for 2 hours in MSC culture media. Splenocytes were isolated from either BDC2.5 TCR transgenic mice (CD4 T cells specific for BDC2.5 mimotope on MHCII) or from NY8.3 TCR transgenic mice (CD8 T cells specific for IGRP

peptide on MHCI) and labeled using CellTrace Violet (cell proliferation kit, Invitrogen, San Diego, CA, USA) for cell proliferation quantification by CellTrace dilution. The MSC media were removed. Splenocytes were added at a density of 100,000 per well into each well on top of the MSCs using culture medium for splenocytes. Splenocytes were stimulated either with BDC2.5 (5 μg/ml) peptide (sequence: RTRPLWVRME) or with IGRP (0.1 μg/ml) peptide (sequence: VYLKTNVFL) in the presence of MSCs or eMSCs for 3 days. After 3 days' coculture, the splenocytes were harvested and stained for flow cytometry analysis using LIVE/DEAD Fixable Dead Cell Stain (near infrared, Invitrogen, L34975) and antibodies against the following surface markers: anti-mouse CD3 (BD Biosciences, 555274), anti-mouse CD4 (eBioscience, 56004182), anti-mouse CD8 (BD Biosciences, 551182), anti-mouse CD44 (BD Biosciences, 582464), anti-mouse CD25 (BD Biosciences, 552880), and granzyme B (BioLegend, 515406). Live, $CD3^+CD4^-CD8^+$, and $CD3^+CD4^+CD8^-$ T cell subpopulations were identified, and their proliferation in vitro was quantified by CellTrace dilution. Activation was determined by CD25 and CD44 up-regulation for CD4 and by CD25, CD44, and granzyme B up-regulation for CD8. Flow cytometry was performed with a CytoFlex S flow cytometer (Beckman Coulter, Brea, CA, USA), and data were analyzed with FlowJo (Tree Star Inc., Ashland, Oregon, USA).

Live and dead staining

Fifty islets without MSCs, with MSC spheroids, or with eMSC spheroids were cultured in 3 ml of RPMI 1640 complete media for 24 hours in nonadherent 25-mm^2 culture dishes. After culture, islets were handpicked and stained by calcein-AM (green, live) and ethidium homodimer (red, dead) according to the manufacturer's protocol (R37601, Thermo Fisher Scientific). Fluorescent microscopic images were taken using a digital inverted microscope (EVOS FL Cell Imaging System). Quantification of the percentage of live cells in islets was carried out by calculating the intensity of fluorescence using ImageJ.

In vitro GSIS

Fifty islets without MSCs, with MSC spheroids, or with eMSC spheroids were cultured in 3 ml of RPMI 1640 complete media for 24 hours in nonadherent 25-mm^2 culture dishes. After culture, islets were handpicked and incubated in prewarmed Krebs-Ringer bicarbonate solution supplemented with 25 mM Hepes, 1 mM L-GlutaMAX, 0.1% BSA, and 2.8 mM D-glucose for 30 min at 37°C, 5% CO^2 for calibration, and then incubated for 1 hour with 2.8 mM or 16.7 mM D-glucose under the same condition. The supernatant was collected and frozen for future analysis. The insulin content in the supernatant was quantified by mouse insulin ELISA kit (ALPCO) according to the manufacturer's specification. Absorbance of reaction solution at 450 nm was measured in the Synergy plate reader (Biotek). The SI was calculated as the ratio of insulin secretion at high glucose (16.7 mM) to that at low glucose (2.8 mM).

Bioluminescent imaging

At different time points after transplantation, the mice were injected with luciferin (150 mg/kg body weight; PerkinElmer, 122799) and imaged with the IVIS Spectrum System (PerkinElmer) at the Biotechnology Resource Center at Cornell.

Isolation of rodent pancreatic islets

Mouse pancreatic islets were isolated from 8-week-old male BALB/c mice or L2G85 mice. One bottle of collagenase (Vitacyte, CIzyme RI, 005-1030) was reconstituted in 30 ml of M199 media (Gibco, USA). The bile duct was cannulated with a 27-gauge needle, and the pancreas was distended with cold collagenase. The perfused pancreases were then removed and digested in a 37°C water bath for 21 min. Islets were centrifuged in lymphocyte separation medium (Corning, 25-072-CV)/M199 media gradient in 1750 rcf for 20 min at 4°C. Purified islets were hand-counted by aliquot under a stereomicroscope (Olympus SZ61). Detailed procedures of isolation and purification were described in previous publications (*5*, *77*).

Chemically induced diabetic mouse model

To create diabetic mice, mice were injected intraperitoneally with freshly prepared STZ (Sigma-Aldrich, 130 mg/kg body weight) solution (13 mg/ml in 5 mM sodium citrate buffer solution). A small drop of blood was collected from the tail vein using a lancet and tested using a commercial glucometer (Contour next, Ascensia Diabetes Care, NJ). Only mice whose nonfasted blood glucose concentrations were above 300 mg/dl with two consecutive measurements were considered diabetic and underwent transplantation.

Injection of 4T1 cell line

The 4T1 cells were detached from the culture dish using TrypLE. Half-million native 4T1 cells or modified 4T1 cells were suspended in 50 μl of 50% Matrigel (Corning, 354277). Then, cell suspension was transferred to a 0.5-ml syringe and injected into the muscle of the right hindlimb.

Preparation of islet samples for transplant

Under an inverted microscope, islets were hand-picked and transferred into each microcentrifuge tube (150 to 200 IEQ/tube for syngeneic islet transplantation; 500 to 600 IEQ/tube for allogeneic islet transplantation). MSC or eMSC spheroids (500 to 600) were added into each tube. The samples were centrifuged and washed with PBS to remove the culture medium. The islet and cell pellets in each tube were resuspended in 50 μl of PBS. Then, the islet and cell suspensions in each tube were loaded into polyethylene (PE) tubing (BD Biosciences, 63018-668). The PE tubing was centrifuged at 1000 rpm for 10 min and placed on ice.

Cell transplantation in kidney capsule

The diabetic mice were anesthetized with isoflurane, and the left flank of the mouse was shaved. The surgical area was sanitized with povidone iodine swab and ethanol swab. The left kidney was located, and a small incision was made in the skin and then in the peritoneum to expose the left kidney. The kidney was popped out of the peritoneum when a slight pressure was applied to the incision. The PE tubing was carefully slid under the kidney capsule making a small pocket to hold the islet samples. The islets with or without cell samples were slowly loaded into the kidney capsule. The kidney was gently put back into the peritoneum before closing the incision with suture and skin staples. After surgery, mice were monitored twice a week, and blood glucose was detected. A total of 500 to 600 GFP/luciferase MSC spheroids or the corresponding number of MSC single cells were transplanted in the kidney capsule of healthy C57BL/6 mice using the method described above.

Intraperitoneal glucose tolerance test

Mice were fasted overnight before receiving an intraperitoneal glucose bolus (2 g/kg body weight). The healthy mice and diabetic mice

were used as positive control and negative control, respectively. Blood glucose was monitored at regular intervals (time: 0, 15, 30, 60, 90, and 120 min) after injection, allowing for the area under the curve to be calculated and analyzed between groups.

Immune profiling

The following procedures were previously described (*5*). BALB/c islets (500 IEQ) without MSCs or with MSC spheroids or with eMSC spheroids were transplanted in diabetic C57BL/6 mice in the kidney capsule. Eight days after transplantation, the kidney transplanted with islets was retrieved. The tissue containing islets was sliced from the kidney using scissors and digested with type I collagenase (1 mg/ml) (Worthington Biochemical Corporation, LS004194) for 1 hour in an incubator. The digestion was stopped by adding cell culture medium containing 10% FBS. The digested tissue was smashed, and the cell solution was filtered through a Falcon 40-μm strainer (Corning, 431750) to obtain single cells. Cells were centrifuged at 1000 rpm for 5 min. Supernatant was discarded, and cells were washed with PBS solution to remove the remaining FBS. The cells were stained with the Zombie Yellow Fixable Viability Kit (BioLegend, 423103) following the manufacturer's instruction. Cells were washed with 2 ml of cell-staining buffer (BioLegend, 420201) and centrifuged into a pellet. Fc receptors were blocked by preincubating cells with TruStain FcX PLUS (anti-mouse CD16/32) antibody (BioLegend, 156603) in 100 μl of cell-staining buffer for 5 min on ice. Then, cells were labeled with mixed antibodies (table S4) on ice for 30 min. The cells were washed twice with 2 ml of cell-staining buffer by centrifugation at 350 rcf for 5 min. The cells were further stained with Foxp3 using the Foxp3/transcription factor staining buffer set (Thermo Fisher Scientific, 00-5523-00) according to the manufacturer's instruction. Samples stained with fluorescence minus one for intracellular staining were run with every collection. UltraComp eBeads Compensation Beads (Thermo Fisher Scientific, 01-2222-41) incubated with each antibody following the manufacturer's instruction were used for compensation. Last, stained cells were analyzed using an Attune NxT flow cytometer (Thermo Fisher Scientific). The data were analyzed by FlowJo software v10.7.

Histological analysis

The following procedures were previously described (*5*). The implants and the spleens were harvested from the mice and fixed in 10% formalin, dehydrated with graded ethanol solutions, embedded in paraffin, and sectioned by Cornell Histology Core Facility. The samples were sliced on a microtome at a thickness of 5 μm. The sections were stained with H&E and then imaged by a microscope (IN200TC, Amscope). To conduct immunofluorescent staining, the histological slides were deparaffinized followed by antigen retrieval as described before (*78*). Nonspecific binding was blocked via incubation with 5% donkey serum (Sigma-Aldrich, S30-M) for 1 hour at room temperature. Sections were decanted and incubated with primary antibodies overnight at 4°C. The sections were then washed and incubated with the fluorescence-conjugated secondary antibodies for 1 hour at room temperature. Nuclei were labeled with DAPI, and slides were covered with fluorescent mounting medium (Sigma-Aldrich, F6057). Last, the sections were imaged through confocal microscopy (FV1000, Olympus, Japan). The antibodies used here are listed in table S5. The density of $CD3^+$, $CD4^+$, $CD8^+$, $Foxp3^+$, and $PD\text{-}1^+$ cells and the ratio of $CD3^+$ to insulin-producing (INS^+) cells were analyzed using ImageJ software.

Statistical analysis

Unless otherwise stated, data were expressed as means ± SD. For comparisons between two groups, means were compared using two-tailed Student's *t* tests. Comparisons between multiple groups were performed by analysis of variance (ANOVA), followed by Tukey's post hoc analysis. Survival curves were analyzed using a Mantel-Cox test. Sample size, including number of mice per group, was chosen to ensure adequate power and was based on literature and historical data. Treated diabetic animals that did not reverse diabetes after allogeneic islet transplantation within 10 days (defined as three consecutive blood glucose readings >300 mg/dl) were excluded from analysis as the failure was not attributable entirely to immune rejection but possibly to variations in islet quality and size, cell numbers, surgery, and other factors (*27*, *56*). All statistical analyses were performed using GraphPad Prism v.8 software (GraphPad Software Inc.). The level of significance was assessed starting at $P < 0.05$.

SUPPLEMENTARY MATERIALS

Supplementary material for this article is available at https://science.org/doi/10.1126/sciadv.abn0071

View/request a protocol for this paper from *Bio-protocol*.

REFERENCES AND NOTES

1. A. M. J. Shapiro, C. Ricordi, B. J. Hering, H. Auchincloss, R. Lindblad, R. P. Robertson, A. Secchi, M. D. Brendel, T. Berney, D. C. Brennan, E. Cagliero, R. Alejandro, E. A. Ryan, B. DiMercurio, P. Morel, K. S. Polonsky, J.-A. Reems, R. G. Bretzel, F. Bertuzzi, T. Froud, R. Kandaswamy, D. E. R. Sutherland, G. Eisenbarth, M. Segal, J. Preiksaitis, G. S. Korbutt, F. B. Barton, L. Viviano, V. Seyfert-Margolis, J. Bluestone, J. R. T. Lakey, International trial of the Edmonton protocol for islet transplantation. *N. Engl. J. Med.* **355**, 1318–1330 (2006).
2. A. M. J. Shapiro, J. R. T. Lakey, E. A. Ryan, G. S. Korbutt, E. Toth, G. L. Warnock, N. M. Kneteman, R. V. Rajotte, Islet transplantation in seven patients with type 1 diabetes mellitus using a glucocorticoid-free immunosuppressive regimen. *N. Engl. J. Med.* **343**, 230–238 (2000).
3. I. Hernández-Fisac, J. Pizarro-Delgado, C. Calle, M. Marques, A. Sánchez, A. Barrientos, J. Tamarit-Rodriguez, Tacrolimus-induced diabetes in rats courses with suppressed insulin gene expression in pancreatic islets. *Am. J. Transplant.* **7**, 2455–2462 (2007).
4. R. Arnold, B. A. Pussell, T. J. Pianta, C. S.-Y. Lin, M. C. Kiernan, A. V. Krishnan, Association between calcineurin inhibitor treatment and peripheral nerve dysfunction in renal transplant recipients. *Am. J. Transplant.* **13**, 2426–2432 (2013).
5. X. Wang, K. G. Maxwell, K. Wang, D. T. Bowers, J. A. Flanders, W. Liu, L.-H. Wang, Q. Liu, C. Liu, A. Naji, Y. Wang, B. Wang, J. Chen, A. U. Ernst, J. M. Melero-Martin, J. R. Millman, M. Ma, A nanofibrous encapsulation device for safe delivery of insulin-producing cells to treat type 1 diabetes. *Sci. Transl. Med.* **13**, eabb4601 (2021).
6. Q. Liu, X. Wang, A. Chiu, W. Liu, S. Fuchs, B. Wang, L. Wang, J. Flanders, Y. Zhang, K. Wang, J. M. Melero-Martin, M. Ma, A Zwitterionic polyurethane nanoporous device with low foreign-body response for islet encapsulation. *Adv Mater* **33**, e2102852 (2021).
7. S. Fuchs, A. U. Ernst, L.-H. Wang, K. Shariati, X. Wang, Q. Liu, M. Ma, Hydrogels in emerging technologies for type 1 diabetes. *Chem. Rev.* **121**, 11458–11526 (2021).
8. A. U. Ernst, D. T. Bowers, L.-H. Wang, K. Shariati, M. D. Plesser, N. K. Brown, T. Mehrabyan, M. Ma, Nanotechnology in cell replacement therapies for type 1 diabetes. *Adv. Drug Deliver Rev.* **139**, 116–138 (2019).
9. X. Wang, N. K. Brown, B. Wang, K. Shariati, K. Wang, S. Fuchs, J. M. Melero-Martin, M. Ma, Local immunomodulatory strategies to prevent allo-rejection in transplantation of insulin-producing cells. *Adv. Sci.* **8**, 2003708 (2021).
10. F. G. Lakkis, R. I. Lechler, Origin and biology of the allogeneic response. *Cold Spring Harb. Perspect Med.* **3**, a014993 (2013).
11. J. L. Zakrzewski, M. R. M. van den Brink, J. A. Hubbell, Overcoming immunological barriers in regenerative medicine. *Nat. Biotechnol.* **32**, 786–794 (2014).
12. T. Okazaki, S. Chikuma, Y. Iwai, S. Fagarasan, T. Honjo, A rheostat for immune responses: The unique properties of PD-1 and their advantages for clinical application. *Nat. Immunol.* **14**, 1212–1218 (2013).
13. J. Yang, L. V. Riella, S. Chock, T. Liu, X. Zhao, X. Yuan, A. M. Paterson, T. Watanabe, V. Vanguri, H. Yagita, M. Azuma, B. R. Blazar, G. J. Freeman, S. J. Rodig, A. H. Sharpe, A. Chandraker, M. H. Sayegh, The novel costimulatory programmed death ligand 1/B7.1 Pathway is functional in inhibiting alloimmune responses in vivo. *J. Immunol.* **187**, 1113–1119 (2011).

14. J. Dudler, J. Li, M. Pagnotta, M. Pascual, L. K. von Segesser, G. Vassalli, Gene transfer of programmed death ligand-1.Ig prolongs cardiac allograft survival. *Transplantation* **82**, 1733–1737 (2006).
15. W. Gao, G. Demirci, T. B. Strom, X. C. Li, Stimulating PD-1–negative signals concurrent with blocking CD154 co-stimulation induces long-term islet allograft survival1. *Transplantation* **76**, 994–999 (2003).
16. M. P. Watson, A. J. T. George, D. F. P. Larkin, Differential effects of costimulatory pathway modulation on corneal allograft survival. *Invest. Ophthalmol. Vis. Sci.* **47**, 3417–3422 (2006).
17. F. J. Dumont, Technology evaluation: Abatacept, Bristol-Myers Squibb. *Curr. Opin. Mol. Ther.* **6**, 318–330 (2004).
18. C. P. Larsen, E. T. Elwood, D. Z. Alexander, S. C. Ritchie, R. Hendrix, C. Tucker-Burden, H. R. Cho, A. Aruffo, D. Hollenbaugh, P. S. Linsley, K. J. Winn, T. C. Pearson, Long-term acceptance of skin and cardiac allografts after blocking CD40 and CD28 pathways. *Nature* **381**, 434–438 (1996).
19. L. A. Turka, P. S. Linsley, H. Lin, W. Brady, J. M. Leiden, R. Q. Wei, M. L. Gibson, X. G. Zheng, S. Myrdal, D. Gordon, T-cell activation by the CD28 ligand B7 is required for cardiac allograft rejection in vivo. *Proc. Natl. Acad. Sci. U.S.A.* **89**, 11102–11105 (1992).
20. H. Lin, S. F. Bolling, P. S. Linsley, R. Q. Wei, D. Gordon, C. B. Thompson, L. A. Turka, Long-term acceptance of major histocompatibility complex mismatched cardiac allografts induced by CTLA4Ig plus donor-specific transfusion. *J. Exp. Med.* **178**, 1801–1806 (1993).
21. W. Li, L. Lu, Z. Wang, L. Wang, J. J. Fung, A. W. Thomson, S. Qian, Costimulation blockade promotes the apoptotic death of graft-infiltrating t cells and prolongs survival of hepatic allografts from flt3l-treated donors1. *Transplantation* **72**, 1423–1432 (2001).
22. H. M. Tran, P. W. Nickerson, A. C. Restifo, M. A. Ivis-Woodward, A. Patel, R. D. Allen, T. B. Strom, P. J. O'Connell, Distinct mechanisms for the induction and maintenance of allograft tolerance with CTLA4-Fc treatment. *J. Immunol.* **159**, 2232–2239 (1997).
23. U. Grohmann, C. Orabona, F. Fallarino, C. Vacca, F. Calcinaro, A. Falorni, P. Candeloro, M. L. Belladonna, R. Bianchi, M. C. Fioretti, P. Puccetti, CTLA-4–Ig regulates tryptophan catabolism in vivo. *Nat. Immunol.* **3**, 1097–1101 (2002).
24. M. A. Curran, W. Montalvo, H. Yagita, J. P. Allison, PD-1 and CTLA-4 combination blockade expands infiltrating T cells and reduces regulatory T and myeloid cells within B16 melanoma tumors. *Proc. Natl. Acad. Sci. U.S.A.* **107**, 4275–4280 (2010).
25. B. T. Fife, J. A. Bluestone, Control of peripheral T-cell tolerance and autoimmunity via the CTLA-4 and PD-1 pathways. *Immunol. Rev.* **224**, 166–182 (2008).
26. E. Özkaynak, L. Wang, A. Goodearl, K. McDonald, S. Qin, T. O'Keefe, T. Duong, T. Smith, J.-C. Gutierrez-Ramos, J. B. Rottman, A. J. Coyle, W. W. Hancock, Programmed death-1 targeting can promote allograft survival. *J. Immunol.* **169**, 6546–6553 (2002).
27. M. M. Coronel, K. E. Martin, M. D. Hunckler, G. Barber, E. B. O'Neill, J. D. Medina, E. Opri, C. A. McClain, L. Batra, J. D. Weaver, H. S. Lim, P. Qiu, E. A. Botchwey, E. S. Yolcu, H. Shirwan, A. J. García, Immunotherapy via PD-L1–presenting biomaterials leads to long-term islet graft survival. *Sci. Adv.* **6**, eaba5573 (2020).
28. M. M. E. Khatib, T. Sakuma, J. M. Tonne, M. S. Mohamed, S. J. Holditch, B. Lu, Y. C. Kudva, Y. Ikeda, β-Cell-targeted blockage of PD1 and CTLA4 pathways prevents development of autoimmune diabetes and acute allogeneic islets rejection. *Gene Ther.* **22**, 430–438 (2015).
29. L. Batra, P. Shrestha, H. Zhao, K. B. Woodward, A. Togay, M. Tan, O. Grimany-Nuno, M. T. Malik, M. M. Coronel, A. J. García, H. Shirwan, E. S. Yolcu, Localized immunomodulation with PD-L1 results in sustained survival and function of allogeneic islets without chronic immunosuppression. *J. Immunol.* **204**, 2840–2851 (2020).
30. R. Li, J. Lee, M. Kim, V. Liu, M. Moulik, H. Li, Q. Yi, A. Xie, W. Chen, L. Yang, Y. Li, T. H. Tsai, K. Oka, L. Chan, V. Yechoor, PD-L1–driven tolerance protects neurogenin3-induced islet neogenesis to reverse established type 1 diabetes in NOD mice. *Diabetes* **64**, 529–540 (2014).
31. P. Bianco, X. Cao, P. S. Frenette, J. J. Mao, P. G. Robey, P. J. Simmons, C.-Y. Wang, The meaning, the sense and the significance: Translating the science of mesenchymal stem cells into medicine. *Nat. Med.* **19**, 35–42 (2013).
32. C. L. Rackham, A. E. Vargas, R. G. Hawkes, S. Amisten, S. J. Persaud, A. L. F. Austin, A. J. F. King, P. M. Jones, Annexin A1 is a key modulator of mesenchymal stromal cell–mediated improvements in islet function. *Diabetes* **65**, db150990 (2015).
33. E.-J. Jung, S.-C. Kim, Y.-M. Wee, Y.-H. Kim, M. Y. Choi, S.-H. Jeong, J. Lee, D.-G. Lim, D.-J. Han, Bone marrow-derived mesenchymal stromal cells support rat pancreatic islet survival and insulin secretory function in vitro. *Cytotherapy* **13**, 19–29 (2011).
34. T. Ito, S. Itakura, I. Todorov, J. Rawson, S. Asari, J. Shintaku, I. Nair, K. Ferreri, F. Kandeel, Y. Mullen, Mesenchymal stem cell and islet co-transplantation promotes graft revascularization and function. *Transplantation* **89**, 1438–1445 (2010).
35. G. Yoshimatsu, N. Sakata, H. Tsuchiya, T. Minowa, T. Takemura, H. Morita, T. Hata, M. Fukase, T. Aoki, M. Ishida, F. Motoi, T. Naitoh, Y. Katayose, S. Egawa, M. Unno, The co-transplantation of bone marrow–derived mesenchymal stem cells reduced inflammation in intramuscular islet transplantation. *PLOS ONE* **10**, e0117561 (2015).
36. J. Cai, Z. Wu, X. Xu, L. Liao, J. Chen, L. Huang, W. Wu, F. Luo, C. Wu, A. Pugliese, A. Pileggi, C. Ricordi, J. Tan, Umbilical cord mesenchymal stromal cell with autologous bone marrow cell transplantation in established type 1 diabetes: A pilot randomized controlled open-label clinical study to assess safety and impact on insulin secretion. *Diabetes Care* **39**, 149–157 (2015).
37. A. Uccelli, L. Moretta, V. Pistoia, Mesenchymal stem cells in health and disease. *Nat. Rev. Immunol.* **8**, 726–736 (2008).
38. O. Levy, R. Kuai, E. M. J. Siren, D. Bhere, Y. Milton, N. Nissar, M. D. Biasio, M. Heinelt, B. Reeve, R. Abdi, M. Alturki, M. Fallatah, A. Almalik, A. H. Alhasan, K. Shah, J. M. Karp, Shattering barriers toward clinically meaningful MSC therapies. *Sci. Adv.* **6**, eaba6884 (2020).
39. M. M. Lalu, L. McIntyre, C. Pugliese, D. Fergusson, B. W. Winston, J. C. Marshall, J. Granton, D. J. Stewart; Canadian Critical Care Trials Group, Safety of cell therapy with mesenchymal stromal cells (SafeCell): A systematic review and meta-analysis of clinical trials. *PLOS ONE* **7**, e47559 (2012).
40. H. Niess, J. C. von Einem, M. N. Thomas, M. Michl, M. K. Angele, R. Huss, C. Günther, P. J. Nelson, C. J. Bruns, V. Heinemann, Treatment of advanced gastrointestinal tumors with genetically modified autologous mesenchymal stromal cells (TREAT-ME1): Study protocol of a phase I/II clinical trial. *BMC Cancer* **15**, 237 (2015).
41. S. Forbes, A. R. Bond, K. L. Thirlwell, P. Burgoyne, K. Samuel, J. Noble, G. Borthwick, D. Colligan, N. W. A. McGowan, P. S. Lewis, A. R. Fraser, J. C. Mountford, R. N. Carter, N. M. Morton, M. L. Turner, G. J. Graham, J. D. M. Campbell, Human umbilical cord perivascular cells improve human pancreatic islet transplant function by increasing vascularization. *Sci. Transl. Med.* **12**, eaan5907 (2020).
42. J. A. Bluestone, E. W. S. Clair, L. A. Turka, CTLA4Ig: Bridging the basic immunology with clinical application. *Immunity* **24**, 233–238 (2006).
43. D. S. Chen, I. Mellman, Elements of cancer immunity and the cancer-immune set point. *Nature* **541**, 321–330 (2017).
44. Z. Rong, M. Wang, Z. Hu, M. Stradner, S. Zhu, H. Kong, H. Yi, A. Goldrath, Y.-G. Yang, Y. Xu, X. Fu, An effective approach to prevent immune rejection of human ESC-derived allografts. *Cell Stem Cell* **14**, 121–130 (2014).
45. E. Yoshihara, C. O'Connor, E. Gasser, Z. Wei, T. G. Oh, T. W. Tseng, D. Wang, F. Cayabyab, Y. Dai, R. T. Yu, C. Liddle, A. R. Atkins, M. Downes, R. M. Evans, Immune-evasive human islet-like organoids ameliorate diabetes. *Nature* **586**, 606–611 (2020).
46. B. J. González, R. J. Creusot, M. Sykes, D. Egli, How safe are universal pluripotent stem cells? *Cell Stem Cell* **26**, 307–308 (2020).
47. K. Wang, L.-Y. Yu, L.-Y. Jiang, H.-B. Wang, C.-Y. Wang, Y. Luo, The paracrine effects of adipose-derived stem cells on neovascularization and biocompatibility of a macroencapsulation device. *Acta Biomater.* **15**, 65–76 (2015).
48. S. H. Bhang, S.-W. Cho, W.-G. La, T.-J. Lee, H. S. Yang, A.-Y. Sun, S.-H. Baek, J.-W. Rhie, B.-S. Kim, Angiogenesis in ischemic tissue produced by spheroid grafting of human adipose-derived stromal cells. *Biomaterials* **32**, 2734–2747 (2011).
49. C. L. Stabler, Y. Li, J. M. Stewart, B. G. Keselowsky, Engineering immunomodulatory biomaterials for type 1 diabetes. *Nat. Rev. Mater.* **4**, 429–450 (2019).
50. T. M. Brusko, H. A. Russ, C. L. Stabler, Strategies for durable β cell replacement in type 1 diabetes. *Science* **373**, 516–522 (2021).
51. M. E. Keir, M. J. Butte, G. J. Freeman, A. H. Sharpe, PD-1 and its ligands in tolerance and immunity. *Annu. Rev. Immunol.* **26**, 677–704 (2008).
52. T. Yamazaki, H. Akiba, H. Iwai, H. Matsuda, M. Aoki, Y. Tanno, T. Shin, H. Tsuchiya, D. M. Pardoll, K. Okumura, M. Azuma, H. Yagita, Expression of programmed death 1 ligands by murine T cells and APC. *J. Immunol.* **169**, 5538–5545 (2002).
53. S. Hirata, S. Senju, H. Matsuyoshi, D. Fukuma, Y. Uemura, Y. Nishimura, Prevention of experimental autoimmune encephalomyelitis by transfer of embryonic stem cell-derived dendritic cells expressing myelin oligodendrocyte glycoprotein peptide along with TRAIL or programmed death-1 ligand. *J. Immunol.* **174**, 1888–1897 (2005).
54. L. Maxwell, J. A. Singh, Abatacept for rheumatoid arthritis. *Cochrane Database Syst. Rev.* **2009**, CD007277 (2009).
55. H. Wang, C. Strange, P. J. Nietert, J. Wang, T. L. Turnbull, C. Cloud, S. Owczarski, B. Shuford, T. Duke, G. Gilkeson, L. Luttrell, K. Hermayer, J. Fernandes, D. B. Adams, K. A. Morgan, Autologous mesenchymal stem cell and islet cotransplantation: Safety and efficacy. *Stem Cell Transl. Med.* **7**, 11–19 (2017).
56. D. M. Headen, K. B. Woodward, M. M. Coronel, P. Shrestha, J. D. Weaver, H. Zhao, M. Tan, M. D. Hunckler, W. S. Bowen, C. T. Johnson, L. Shea, E. S. Yolcu, A. J. García, H. Shirwan, Local immunomodulation with Fas ligand–engineered biomaterials achieves allogeneic islet graft acceptance. *Nat. Mater.* **17**, 732–739 (2018).
57. M. Skoumal, K. B. Woodward, H. Zhao, F. Wang, E. S. Yolcu, R. M. Pearson, K. R. Hughes, A. J. García, L. D. Shea, H. Shirwan, Localized immune tolerance from FasL-functionalized PLG scaffolds. *Biomaterials* **192**, 271–281 (2018).
58. C. Raffin, L. T. Vo, J. A. Bluestone, Treg cell-based therapies: Challenges and perspectives. *Nat. Rev. Immunol.* **20**, 158–172 (2019).
59. L. M. R. Ferreira, Y. D. Muller, J. A. Bluestone, Q. Tang, Next-generation regulatory T cell therapy. *Nat. Rev. Drug Discov.* **18**, 749–769 (2019).

60. J. A. Bluestone, J. H. Buckner, M. Fitch, S. E. Gitelman, S. Gupta, M. K. Hellerstein, K. C. Herold, A. Lares, M. R. Lee, K. Li, W. Liu, S. A. Long, L. M. Masiello, V. Nguyen, A. L. Putnam, M. Rieck, P. H. Sayre, Q. Tang, Type 1 diabetes immunotherapy using polyclonal regulatory T cells. *Sci. Transl. Med.* **7**, 315ra189 (2015).
61. N. Marek-Trzonkowska, M. Myśliwiec, A. Dobyszuk, M. Grabowska, I. Derkowska, J. Juścińska, R. Owczuk, A. Szadkowska, P. Witkowski, W. Młynarski, P. Jarosz-Chobot, A. Bossowski, J. Siebert, P. Trzonkowski, Therapy of type 1 diabetes with $CD4^+CD25^{high}CD127$-regulatory T cells prolongs survival of pancreatic islets—Results of one year follow-up. *Clin. Immunol.* **153**, 23–30 (2014).
62. J. G. Graham, X. Zhang, A. Goodman, K. Pothoven, J. Houlihan, S. Wang, R. M. Gower, X. Luo, L. D. Shea, PLG scaffold delivered antigen-specific regulatory T cells induce systemic tolerance in autoimmune diabetes. *Tissue Eng Part A.* **19**, 1465–1475 (2013).
63. N. Takemoto, S. Konagaya, R. Kuwabara, H. Iwata, Coaggregates of regulatory T cells and islet cells allow long-term graft survival in liver without immunosuppression. *Transplantation* **99**, 942–947 (2015).
64. H. T. Lau, M. Yu, A. Fontana, C. J. Stoeckert, Prevention of islet allograft rejection with engineered myoblasts expressing FasL in mice. *Science* **273**, 109–112 (1996).
65. G. T. Motz, S. P. Santoro, L.-P. Wang, T. Garrabrant, R. R. Lastra, I. S. Hagemann, P. Lal, M. D. Feldman, F. Benencia, G. Coukos, Tumor endothelium FasL establishes a selective immune barrier promoting tolerance in tumors. *Nat. Med.* **20**, 607–615 (2014).
66. N. P. Restifo, Not so Fas: Re-evaluating the mechanisms of immune privilege and tumor escape. *Nat. Med.* **6**, 493–495 (2000).
67. R. B. Jalili, F. Forouzandeh, A. M. Rezakhanlou, R. Hartwell, A. Medina, G. L. Warnock, B. Larijani, A. Ghahary, Local expression of indoleamine 2,3 dioxygenase in syngeneic fibroblasts significantly prolongs survival of an engineered three-dimensional islet allograft. *Diabetes* **59**, 2219–2227 (2010).
68. W. Chen, IDO: More than an enzyme. *Nat. Immunol.* **12**, 809–811 (2011).
69. A. Mellor, Indoleamine 2,3 dioxygenase and regulation of T cell immunity. *Biochem. Biophys. Res. Commun.* **338**, 20–24 (2005).
70. Z. Chinn, M. H. Stoler, A. M. Mills, PD-L1 and IDO expression in cervical and vulvar invasive and intraepithelial squamous neoplasias: Implications for combination immunotherapy. *Histopathology* **74**, 256–268 (2019).
71. M. L. Zhang, M. Kem, M. J. Mooradian, J.-P. Eliane, T. G. Huynh, A. J. Iafrate, J. F. Gainor, M. Mino-Kenudson, Differential expression of PD-L1 and IDO1 in association with the immune microenvironment in resected lung adenocarcinomas. *Mod. Pathol.* **32**, 511–523 (2019).
72. E. Eggenhofer, F. Luk, M. H. Dahlke, M. J. Hoogduijn, The life and fate of mesenchymal stem cells. *Front. Immunol.* **5**, 148 (2014).
73. E. Eggenhofer, V. Benseler, A. Kroemer, F. C. Popp, E. K. Geissler, H. J. Schlitt, C. C. Baan, M. H. Dahlke, M. J. Hoogduijn, Mesenchymal stem cells are short-lived and do not migrate beyond the lungs after intravenous infusion. *Front. Immunol.* **3**, 297 (2012).
74. M. B. Preda, C. A. Neculachi, I. M. Fenyo, A.-M. Vacaru, M. A. Publik, M. Simionescu, A. Burlacu, Short life span of syngeneic transplanted MSC is a consequence of in vivo apoptosis and immune cell recruitment in mice. *Cell Death Dis.* **12**, 566 (2021).
75. L. Li, X. Chen, W. E. Wang, C. Zeng, How to improve the survival of transplanted mesenchymal stem cell in ischemic heart? *Stem Cells Int.* **2016**, 9682757 (2016).
76. X. Hu, S. P. Yu, J. L. Fraser, Z. Lu, M. E. Ogle, J.-A. Wang, L. Wei, Transplantation of hypoxia-preconditioned mesenchymal stem cells improves infarcted heart function via enhanced survival of implanted cells and angiogenesis. *J. Thorac. Cardiovasc. Surg.* **135**, 799–808 (2008).
77. K. Wang, X. Wang, C. Han, L. Chen, Y. Luo, Scaffold-supported transplantation of islets in the epididymal fat pad of diabetic mice. *J. Vis. Exp.* 54995 (2017).
78. X. Wang, K. Wang, W. Zhang, M. Qiang, Y. Luo, A bilaminated decellularized scaffold for islet transplantation: Structure, properties and functions in diabetic mice. *Biomaterials* **138**, 80–90 (2017).

Acknowledgments: We thank J. March, T. Walter, and B. Barstow for helping with real-time PCR. We thank T. Feng for helping with Western blot. We thank A. August and C. Limper for helping with immune profiling. We thank G. Koretzky for giving advice on the project. We thank Cornell Histology Core Facility for the histological cross-sectioning and staining. We thank Cornell Flow Cytometry Core Facility for the technical support. We thank Cornell BRC Imaging Facility (NIH S10OD025049) for data acquired with IVIS Spectrum optical imager and especially T. Abratte for the technical support. We thank S. Hu for the help with the paper revision. **Funding:** This work was supported by NIH grant 1R01DK105967-01A1 (to M.M.), the Juvenile Diabetes Research Foundation 2-SRA-2018-472-S-B (to M.M.), the Novo Nordisk Company (to M.M.), and the Hartwell Foundation (to M.M.). **Author contributions:** Conceptualization: X.W. and M.M. Methodology: X.W., B.W., and A.C. Investigation: X.W., K.W., M.Y., D.V., and X.H. Visualization: X.W. Supervision: X.W. and M.M. Writing—original draft: X.W. Writing—review and editing: X.W., J.M.M.-M., A.A.T., and M.M. **Competing interests:** X.W. and M.M. are inventors on a patent application (17/502,949) submitted by Cornell University that covers the engineered cells described in this manuscript. All other authors declare that they have no competing interests. **Data and materials availability:** All data needed to evaluate the conclusions in the paper are present in the paper and/or the Supplementary Materials.

Submitted 27 October 2021
Accepted 8 June 2022
Published 22 July 2022
10.1126/sciadv.abn0071